Crosstalk Analysis and Filter Optimization of Single- and Double-Cavity Fabry-Perot Filters

Pierre A. Humblet and Walid M. Hamdy[1]

February 9, 1990

Abstract

Fabry-Perot Filters are major candidates for use as demultiplexers in wavelength division multiple access networks. In this paper we investigate the crosstalk limitations of such filters, compare their performances, and optimize the filter design to minimize the crosstalk degradation.

[1]Both with the Laboratory for Information and Decision Systems, MIT, Cambridge, MA 02139. This work was performed while both authors were at the IBM T. J. Watson Research Center, Yorktown Heights, NY 10598.

1 Introduction

The advent of dense wavelength division multiple access (WDMA) optical networking is contingent upon the development of several key system components. Among the components required for a non-coherent/direct detection implementation of a WDMA system is a tunable optical filter with a sufficiently narrow passband and a sufficiently wide tuning range to allow extremely close channel spacings over the entire low-loss optical bandwidth window. Fabry-Perot (FP) filters show promise of fulfilling these requirements [1],[2].

The use of FP filters in WDMA systems for channel selection has been studied in several papers [3]-[9], but the analysis of the crosstalk degradation of the bit error rate and the power penalty required to overcome it has only been approximately estimated. The purpose of this paper is to analyze, in an exact and unified manner, the crosstalk degradation for several different variations of the basic FP filter, to compare their performances, and to optimize their design parameters.

This paper is organized as follows: In Section 2 we describe the system model and the parameters used throughout this paper, give a brief review of relevant Fabry-Perot equations and terms, and discuss the four different filter structures to be analyzed in this paper. The following four Sections are devoted to the analysis of crosstalk in the cases of a Single-Cavity FP filter, a Double-Pass FP filter, a Two-Stage Double-Cavity FP filter, and a Vernier Double-Cavity FP filter. A discussion of our results and the conclusions are stated in Section 7.

2 Preliminaries

2.1 System Model

The system analyzed in this paper is a wavelength division multiple access system consisting of M connected transmitters and receivers. Each transmitter consists of an on-off modulated fixed-frequency laser, with the "OFF" power level equal to zero (i.e an ideal extinction ratio). We denote by W the system bandwidth in which the transmitter frequencies are equally spaced, thus giving a channel spacing of W/M Hz. All laser linewidths are assumed to be negligible compared to both the channel spacing and the receiver resolution. In addition, any spectrum broadening due to modulation is, for simplicity, neglected. These limitations are further discussed in Section 7.

Each receiver has an optical filter that may be tuned to select any one of the M transmitters. However, the large passband and non-ideal stop-band attenuation of the filter introduce crosstalk from the other $M-1$ channels. Following the filter, a direct detection receiver detects both the filtered signal and the crosstalk, and performs further electronic processing through which receiver, or thermal, noise is added. This noise is independent of the received power level, and can be modeled as additive Gaussian noise. Since this is an Intensity Modulated/Direct Detection system, the receiver noise dominates all other forms of noise (shot noise, laser excess noise, phase noise, etc...) [10], and therefore will be considered as the sole noise source (in addition to the crosstalk interference).

Crosstalk analysis in this system depends on the structure of the optical filter used in each receiver. In this paper we consider only basic Fabry-Perot filters and variations on them. The following subsection is a brief review of the basic equations describing the operation of such filters.

2.2 Fabry-Perot Filter Equations

A Fabry-Perot (FP) filter consists of two highly reflective parallel mirrors with reflection coefficients r_1 and r_2 separated by a distance L, thus forming a cavity. As is the usual case, we take $r_1^2 = r_2^2 = R$ = reflectivity of both mirrors. In addition, for generality, we assume the mirrors to be lossy with loss parameter $A = 1 - R - T$, where T is the transmittance of both mirrors. Intra-cavity losses are ignored.

The *field* transfer function of an FP filter is then given by [11]

$$t(\delta) = (1 - R - A)\sum_{i=0}^{\infty}(Re^{j2\pi\delta})^i \tag{1}$$

where δ is the normalized optical frequency $= 2fnL/c$, so that $t(\delta)$ is periodic in δ with period 1. The quantity $c/2nL$ is commonly referred to as the free spectral range (FSR), where n is the refractive index of the medium between both mirrors, and c the speed of light in vacuum. Phase changes on the mirrors are ignored.

The *power* transfer function is given by

$$\begin{aligned} T_{SC}(\delta) &= t(\delta)t^*(\delta) && (2)\\ &= (1 - \frac{A}{1-R})^2(\frac{1-R}{1+R})\sum_{n=-\infty}^{\infty} R^{|n|}e^{j2\pi n\delta} && (3)\\ &= (1 - \frac{A}{1-R})^2\frac{1}{1 + ((2F/\pi)\sin(\pi\delta))^2} && (4) \end{aligned}$$

where the subscript (SC) denotes single-cavity. F is the *finesse* of the FP filter, defined as $\pi\sqrt{R}/(1-R)$. For large reflectivity values $(1 - R \ll 1)$, $F \approx$ FSR/FWHM where FWHM (Full Width at Half Maximum) is the 3-dB bandwidth of a passband of the FP-filter. F can be further approximated by

$$F \approx -\pi/\ln(R) \tag{5}$$

We term the factor $(1 - A/(1-R))^2$ in (4) as the maximum intrinsic filter transmission. External losses, such as connector and coupling losses, necessarily reduce the effective filter transmission.

2.3 Alternative Fabry-Perot Filter Structures

The above equations were for a *single-cavity* FP filter. Several variations on this standard structure are possible (see Fig. 1):

1. Double-Pass FP Filter: This is a variation on the single-cavity structure, in which the cavity is "re-used" by returning the output of the filter to pass through the cavity another time. [2]

[2] Multiple (> 2) pass filters are theoretically possible [12], but will suffer significant losses, and will thus not be considered here.

2. Two-Stage Double-Cavity FP Filter: In this case, the filter consists of two cavities with equal or comparable F values, but widely different free spectral ranges (and thus widely different FWHM values). We term it "two-stage" since the first filter may be considered as the first, or rough, stage filter with an FSR equal to the system bandwidth that suppresses all far channels, and the second filter as the "fine-stage" filter that provides the required selectivity by suppressing the adjacent channels.

3. Vernier Double-Cavity FP Filter: Here two cavities are also used, but with FSR values such that K FSRs of filter 1 cover $K+1$ FSRs of filter 2, thereby resulting in a much increased effective FSR, with a reduced FWHM.

A plot of a specific case (Single-Cavity finesse = 100) of the transfer functions of the four structures analyzed in this paper is given in Fig. 2, clearly showing the tradeoff between transmission (or attenuation) and selectivity (or FWHM) for the three double cavity structures above.

All of the above three variations require some form of isolation between the two filter sections in order to prevent unwanted resonances. Several methods for achieving this isolation have been discussed in detail in [4] and [11]. Other alternative structures, such as the three-mirror FP filter [4] [12], will not be covered in this paper.

3 Single-Cavity Filters

3.1 Crosstalk PMF & Worst-Case Crosstalk

An exact analysis of crosstalk in the case of single-cavity filters may be performed as follows: We first note that the system bandwidth in this case is just one FSR, to avoid aliasing effects. We assume all users output equally probable "ON" and "OFF" levels in synchronism and with equal peak power (taken as unity). Justification of the synchronism assumption will be given shortly. The output of the filter, centered on the 0^{th} channel due to the i^{th} channel, $0 \leq i \leq M$, is then a random variable with the probability mass function (pmf)

$$P_i = \begin{cases} 0 & \text{prob} = 1/2 \\ T_{SC}(i/M) & \text{prob} = 1/2 \end{cases} \tag{6}$$

where $T_{SC}(\cdot)$ is defined in (4). The resultant crosstalk is then given by

$$C = \sum_{i=1}^{M-1} P_i \tag{7}$$

where the dependence on M and F is suppressed. The pmf of C may be simply obtained by the convolution of the above $M-1$ pmf's. An example of the crosstalk pmf for the case $M = 40, F = 100$ is given in Fig. 3(a), showing its significantly non-Gaussian shape [3]. This is primarily due to the dominance of the closest neighbors in the crosstalk sum. Fig. 3(b) shows the pmf for "OFF" and "ON" levels, with the threshold set at the midpoint, for the case $M = 80$, $F = 100$.

The worst-case crosstalk occurs when all other $M-1$ transmitters are sending "ON" levels, and may be expressed as

$$S_{SC}(M,F) = \sum_{i=1}^{M-1} \frac{1}{1 + ((2F/\pi)\sin(\pi i/M))^2} \tag{8}$$

As can be easily seen, if users were assumed to be perfectly asynchronous, P_i in (6) would consist of two impulses, each of weight 0.25, at 0 and $T_{SC}(i/M)$ *and* a continuous uniform density between those two points with area 0.5. The worst-case crosstalk is identical in both synchronous and asynchronous cases, but the tails of the pmf using the synchronous assumption are larger than those using the asynchronous assumption. Hence synchronism is a worst-case assumption.

In Appendix A, we show that an exact closed-form expression for the worst-case crosstalk is given by

$$S_{SC}(M,F) = M(\frac{1-R}{1+R})(\frac{1+R^M}{1-R^M}) - 1 \tag{9}$$

where R is the mirror reflectivity, whose dependence on F is suppressed. By using (5), (9) can be rewritten in terms of F resulting in, for the case of large F,

$$S_{SC}(M,F) \approx \frac{\pi M}{2F}\text{cotanh}(\frac{\pi M}{2F}) - 1 \tag{10}$$

showing that $S_{SC}(M,F)$ is, for large F, a function of M/F only. This formula is plotted in Fig. 4. For $F = 100$, it is indistinguishable from (9).

Convenient lower and upper bounds for $S_{SC}(M,F)$ can be derived using results given in Appendix B

[3] All convolutions in this paper were performed using a 1024-point FFT

$$\frac{\pi^2(M/F)^2}{12+2\pi(M/F)} \leq S_{SC}(M,F) \leq \frac{\pi^2}{12}(\frac{M}{F})^2 \tag{11}$$

showing that the the worst-case crosstalk grows roughly as $\frac{\pi^2}{12}(M/F)^2$, in agreement with the results in [8].

The value of M/F that gives $S_{SC}(M,F) = 1$ provides an upper bound on the maximum number of users M that can be supported with a finesse F to produce a zero BER, taking into account *only* the crosstalk interference. This bound can be easily computed from (10) to be approximately

$$M < 1.22F$$

which is an overly optimistic bound, since receiver noise was neglected. This is corrected for in the next subsection.

3.2 Probability of Error and Power Penalty Computation

Assuming that the detector output is scaled such that an "ON" results in a unit level, the probability of error taking into account both the crosstalk and the receiver noise can be straightforwardly calculated as

$$P_e = \frac{1}{2}E_C\left\{Q(\frac{\eta - C}{\sigma}) + Q(\frac{1+C-\eta}{\sigma})\right\} \tag{12}$$

where the expectation is taken over all possible values of the crosstalk random variable C. η is the decision threshold, given by

$$\eta = \frac{1+S_{SC}(M,F)}{2} \tag{13}$$

and σ is the receiver noise standard deviation. σ is equal to the ratio of the noise equivalent power to the peak *optical* power. $Q(x)$ is the Q-function defined as

$$Q(x) = \frac{1}{\sqrt{2\pi}}\int_x^\infty e^{-x^2/2}dx$$

Fig. 5 shows the bit error rate P_e, for the case $F = 100$ and a range of M/F ratios versus SNR, where SNR is defined as

$$SNR \triangleq \frac{1}{\sigma} \tag{14}$$

It should be noted that these plots appear to depend only on the *ratio* M/F. Fig. 6 shows the resultant crosstalk power penalty at three different BERs, where crosstalk power penalty is defined as

$$10\log_{10}(\frac{P_n}{P_o})$$

where P_o is the power needed to produce the given BER in the absence of crosstalk, and P_n the new power needed to produce the same BER in the presence of crosstalk. Fig. 6 shows that, for example, for a power penalty of 0.5 dB at a BER of 10^{-9} a maximum of $M \simeq 0.5F$ users may be allowed. The same figure also shows the zero probability of error power penalty, which is just $-10\log_{10}(1 - S_{SC}(M, F))$.

The fact that there is a power penalty indicates that there is a tradeoff between bandwidth efficiency and power efficiency. In local distribution systems, where power efficiency is not critical, it may be appropriate to operate with a large power penalty to support many users even if some devices have bandwidth limitations.

3.3 Effect of Laser Drift

Ideally, one would require all transmitter frequencies to be absolutely stable at their assigned values over time. In reality, however, this is not always the case, and one must take account of this effect.

Fig. 7 shows the degradation of the BER with increased worst-case laser drift for $M = 40, F = 100$, where a worst-case laser drift of D is defined as the case when all the transmitter frequencies drift by D Hz such that the desired transmitter is attenuated while all other frequencies are amplified. D is measured in units of the FWHM of the filter.

3.4 Additional System Degradations

1. *Threshold Setting*

   So far, we have assumed that the threshold is permanently set at $(1 + S_{SC}(M, F))/2$, which is the average received power when all transmitters are active and sending equally likely "ON"-"OFF" signals. This is optimum only for the case when all users are continuously transmitting; that is when there are no idle or "off-line" users. This clearly may not always be the case.

It is tempting to make the threshold slowly adaptive by setting it to the (time-varying) mean received power instead. However, for large $S_{SC}(M,F)$ this can be disastrous when transmitters on adjacent channels become active after having been inactive, unless if inactive transmitters continue transmitting at half power.

It is interesting to note, however, that if η is kept fixed at $(1+S_{SC}(M,F))/2$, then the probability of error can actually *increase* as other transmitters become inactive. In the extreme case when all but one of the transmitters are inactive, the probability of error is given by

$$P_e = \frac{1}{2}\left\{Q(\frac{\eta}{\sigma}) + Q(\frac{1-\eta}{\sigma})\right\}$$

2. *Non-zero Mirror Loss*

   As is evident from (4), the effect of the mirror loss A is an attenuation of the transmission transfer function by a factor $(1-A/(1-R))^2$. It has no effect on the filter finesse F. Thus, all channels are uniformly attenuated, and the SNR will be reduced accordingly. The same comment holds for other sources of attenuation.

3. *Near-Far Effect*

   The near-far effect is an additional degradation that occurs when the desired channel, or transmitted frequency, is attenuated while all other channels are not. Eliminating this effect simply requires an additional power penalty equal to the suffered attenuation.

4. *Nonideal Extinction Ratios*

   We have so far assumed an ideal extinction ratio $r=0$, with r given by $r \triangleq \frac{P(0)}{P(1)}$ one then may easily show that an additional power penalty equal to $10\log_{10}(1/1-r)$ (for peak power) must be paid (i.e the same as that of the single user case). This can be seen by noticing that the received power distribution in this case will be similar to that of Fig. 3(b), but with a translation to the right by $r(1+S_{SC}(M,F))/(1-r)$. This translation does not affect the probability of error.

3.5 Finesse Optimization

From the previous discussion it appears that it is always beneficial to increase the finesse of the filter to accommodate a larger number of users. However, this is not true when intrinsic

filter losses are taken into account. Consider a filter with mirror loss A and reflectivity R. From (4), the intrinsic filter transmission is $(1 - A/(1-R))^2$ which decreases with F. Some insight can be gained by taking the simplified view that a filter designer can vary R while keeping A fixed. We will seek the finesse F that maximizes the quantity

$$\rho = (1 - \frac{A}{1-R})^2(1 - S_{SC}(M,F))$$

where the first factor reflects the transmission and the second factor the crosstalk effect. $-10\log(\rho)$ can be interpreted as the zero probability of error power penalty.

Using the approximations $S_{SC}(M,F) \approx \frac{\pi^2}{12}(\frac{M}{F})^2$ and $1/(1-R) \approx F/\pi$, the problem is then to maximize the quantity

$$(1 - \frac{AF}{\pi})^2(1 - \frac{\pi^2}{12}(\frac{M}{F})^2)$$

over F. Elementary calculus reveals that at the optimal F,

$$(1 - \frac{AF}{\pi}) = 1 - \frac{\pi^2}{12}(\frac{M}{F})^2$$

from which it is easy to show that the optimal finesse is given by

$$F^* = \frac{\pi}{A}\left\{\frac{(AM)^2}{12}\right\}^{1/3}$$

and that the optimum ρ is

$$\rho^* = \left\{1 - (\frac{(MA)^2}{12})^{1/3}\right\}^3$$

The above formulas show that the number of users that can be supported for a given power penalty is inversely proportional to the attenuation coefficient. One can show that this conclusion remains valid even when using the exact value of $S_{SC}(M,F)$ given by (9) as long as F is large.

Fig. 8 shows the dependence of F^* on M, where both are normalized by A^{-1}. In addition, it shows the increase in optimum crosstalk power penalty (in dB) with the number of users M, where M is normalized by A^{-1}. Both curves in Fig. 8 were obtained by numerical maximization of ρ, to avoid using the approximations of R and $S_{SC}(M,F)$ above.

The same method can be applied to determine optimal finesse for arbitrary relationships between A and F, as well as for other FP structures.

4 Double-Pass Filters

4.1 Crosstalk PMF & Worst-Case Crosstalk

Extension of the results of the previous section for the case of the Double-Pass FP filter is quite straightforward, and simply involves the replacement of the transfer function (4) by

$$T_{DP}(\delta) = \frac{1}{(1 + ((2F/\pi)\sin(\pi\delta))^2)^2} \tag{15}$$

where we set A to zero. Thus C, the crosstalk random variable, is still given by (7), but with $T_{SC}(\cdot)$ replaced by $T_{DP}(\cdot)$ in (6).

Fig. 9 shows the crosstalk pmf for the case of $M = 112$ and $F = 100$, where F is the single-pass finesse. It clearly shows that most of the crosstalk is contributed by the adjacent channels.

The worst-case crosstalk for this case is given by

$$S_{DP}(M, F) = \sum_{i=1}^{M-1} \frac{1}{(1 + ((2F/\pi)\sin(\pi i/M))^2)^2} \tag{16}$$

In Appendix C, we show that an exact closed-form expression for $S_{DP}(M, F)$ is

$$S_{DP}(M, F) = (\frac{1-R}{1+R})^2 \frac{M}{(1-R^M)^2}[\frac{(1-R^{2M})(1+R^2)}{1-R^2} + 2MR^M] - 1 \tag{17}$$

where the dependence of R on F is suppressed. After using (5) and some algebra, we can rewrite the above in terms of F

$$\begin{aligned} S_{DP}(M, F) &\approx \frac{\pi M/F}{4(1 - e^{-(\pi M/F)})^2}[1 - e^{-2(\pi M/F)} + 2\frac{\pi M}{F}e^{-(\pi M/F)}] - 1 && (18) \\ &\approx \frac{(\pi M/F)^4}{720}\frac{1 - (\pi M/F) + \frac{15}{28}(\pi M/F)^2 - \frac{17}{84}(\pi M/F)^3 + \ldots}{1 - (\pi M/F) + \frac{7}{12}(\pi M/F)^2 - \frac{1}{4}(\pi M/F)^3 + \ldots} && (19) \\ &\approx \frac{(\pi M/F)^4}{720}(1 - \frac{(\pi M/F)^2}{21} + \frac{(\pi M/F)^4}{560} - \frac{(\pi M/F)^6}{16632} + \ldots) && (20) \end{aligned}$$

where the last power series expansion is valid for $M/F < 2$. Thus for small M/F, the worst case crosstalk grows as $\frac{1}{720}(\pi M/F)^4$, in agreement with results in [8]. The constraint $S_{DP}(M, F) < 1$ results in a zero-error upperbound on M given by approximately

$$M < 2.53F$$

4.2 BER and Power Penalty Computation

Calculation of the BER and crosstalk power penalty involves the same equations used for the single-cavity filter case ((12) and (13)), with the substitution of $S_{DP}(M,F)$ for $S_{SC}(M,F)$.

Fig. 10 shows the BER for $F = 100$ and various M/F values, and Fig. 11 shows the crosstalk power penalty in this case. Comparing Fig. 10 and 11 with Fig. 5 and 6 respectively, one may see that the value of M that can be supported with a double-pass FP filter for a given BER or power penalty is about 2.1 times that allowed using a single-cavity FP filter.

5 Two-stage Double-Cavity Filters

5.1 Transfer Function

The effective transfer function of the two-stage double-cavity filter is given by

$$T_{TS}(\delta) = \frac{1}{1+((2F/\pi)sin(\pi\delta))^2}\frac{1}{1+((2F/\pi)sin(\pi\delta K))^2} \tag{21}$$

where F is the finesse of each stage, and K is the ratio of FSR_1 to FSR_2 ($K \geq 1$), where FSR_1 is equal to the system bandwidth W, as was shown in Fig. 2 with $K = 10$.

If K is too large, the number of secondary peaks becomes large and excessive crosstalk results. If K is too small, however, then to keep the finesses equal each second-stage passband (FWHM) must be increased, thus reducing the effective resolution of the filter. An optimum K exists, and the following subsection investigates the choice of optimum K.

5.2 Ratio Optimization for Worst-case Crosstalk

The worst-case crosstalk of a two-stage FP filter is extremely sensitive to small changes in M, as exhibited in Fig. 12 for the case $F = 100, K = 28$. Peaks occur when transmitter frequencies coincide with the second-stage transmission maxima. One design method for this structure might then be to choose K so that none of the transmitter frequencies coincides with a second-stage transmission peak. Several problems prevent this kind of fine optimization, however. First, the exact transmitter frequencies maybe unknown when designing the filter. Second, since the filter must be tunable, its effective free spectral range is variable, and hence so are the secondary peak locations.

An alternative design criterion is to require that the crosstalk be small for all transmitter frequency configurations in the vicinity of a nominal design point, which is equivalent to minimizing the maximum, or worst-case, crosstalk. As proved in Appendix C, the worst case occurs when there is a transmitter frequency at each secondary peak, i.e, when K divides the number of transmitters M. If both filters have the same reflectivity R and losses are ignored, and if all transmitters have unit peak power, then the maximum crosstalk is upperbounded by the following formula, which is exact when K divides M. It is also plotted in Fig. 12.

$$S_{TS}(M,F,K) = M(\frac{1-R}{1+R})^2(\frac{1}{1-R^M})(\frac{1}{1-R^{M/K}})(\alpha+\beta) - 1 \tag{22}$$

where

$$\alpha = \frac{(1-R^M R^{M/K})(1+RR^K)}{1-RR^K}$$

$$\beta = \frac{(R+R^K)(R^{M/K}-R^M)}{R-R^K}$$

which reduces to (9) for $K = M$ (single cavity) and (17) for $K = 1$ (double-pass). This formula is exact only when K divides M, but is smooth in M and K and will be used for the optimization over K. The optimal K must be in the vicinity of $\sqrt{M}$, since this is where the competing factors $(1 - R^K)$ and $(1 - R^{M/K})$ in the denominator are equal. Assuming this to be the case and M large, we neglect R^M compared to both R^K and $R^{M/K}$, and we approximate $1 + R$ by 2. This yields

$$S_{TS}(M,F,K) \approx M(\frac{1-R}{2})^2(\frac{1+R^{M/K}}{1-R^{M/K}})(\frac{1+R^K}{1-R^K}) - 1 \tag{23}$$

This is minimized by $K = \sqrt{M}$, and the resulting crosstalk is

$$S_{TS}(M,F) \approx M(\frac{1-R}{2})^2(\frac{1+R^{\sqrt{M}}}{1-R^{\sqrt{M}}})^2 - 1 \tag{24}$$

Using the approximations $1 - R \approx \pi/F$ and $R \approx e^{-\pi/F}$ yields

$$S_{TS}(M,F) \approx (\frac{\pi\sqrt{M}}{2F})^2 \mathrm{cotanh}^2(\frac{\pi\sqrt{M}}{2F}) - 1 \tag{25}$$

Thus the zero-error upperbound on M, when $S_{TS}(M,F) = 1$ is found to be

$$M < 0.55F^2$$

Fig. 13 shows the value of K minimizing (22); the ripples are caused by the constraint that K be integer. Fig. 14 displays both the minimum value of (22) and (25).

The first term in (23) is equal to the square of the first term in (10), with $\sqrt{M}/F$ replacing M/F. The bounds in Appendix B can therefore be adapted to this case, revealing

$$S_{TS}(M,F) \approx \frac{\pi^2 M}{6F^2} \approx 1.645\frac{M}{F^2}$$

which is a very good approximation even for large M/F. Thus the worst-case crosstalk in this system with M users and a single filter finesse F grows as $\frac{\pi^2}{6}(M/F^2)$, and is roughly equal to the worst-case crosstalk in the single-cavity filter with $\sqrt{2M}$ users. Note that the behavior of the optimized system in Fig. 14 is quite different from that of a non-optimized filter as that of Fig. 12, and is in fact just the lower envelope of the upper bound curves for different K's. One should note that the filter of Fig. 12 is optimal when M is around 784. The resulting worst-case crosstalk is about 0.12, but the actual crosstalk is very sensitive to the exact value of M as seen in Figures 12 and 14.

5.3 Crosstalk PMF, BER and Power Penalty Computation

The computation of the crosstalk pmf follows exactly the same method as that of the previous two Sections. In this case we have (7) with $T_{TS}(\cdot)$ replacing $T_{SC}(\cdot)$ in (6).

Fig. 15 shows the crosstalk pmf resulting from two cases: $M = 784, F = 100, K = 28$ and $M = 800, F = 100, K = 28$. The former case, even though it uses a smaller M, has a larger worst-case crosstalk $S_{TS}(M,F,K)$. This is since K divides M (i.e it lies on one of the peaks of Fig. 12). One should also note that the shape of the pmf is also dependent on the exact value of M.

Fig. 16 shows the resulting BER with $F = 100$, and several different values of M with $K = \sqrt{M}$. This choice of K makes it likely that these BER curves are worst-case curves. Fig. 17 shows the resulting crosstalk power penalty for several BERs, where the condition $K = \sqrt{M}$ is also used.

6 Vernier Double-Cavity Filters

6.1 Transfer Function

The power transfer function for the general case double cavity filter with FSR_1/FSR_2 ratio equal to K_2/K_1 is

$$T_V(\delta) = \frac{1}{1 + ((2F/\pi)sin(\pi\delta K_1))^2} \frac{1}{1 + ((2F/\pi)sin(\pi\delta K_2))^2} \tag{26}$$

It is necessary that K_1 and K_2 be relatively prime to insure that there be a single frequency in the system bandwidth where both filters transmit maximally. The tradeoff in choosing K_1 and K_2 is as follows. K_1 and K_2 cannot be chosen too large since the number of secondary peaks is equal to $K_1 + K_2 - 1$. In addition, secondary peak separation will be as small as the system bandwidth divided by K_1K_2, which for large K_1 and K_2 may be too small to provide an acceptable attenuation level. On the other hand, having large K_1 and K_2 leads to a narrower FWHM of the individual filters and thus of the combined filter response. The rolloff of the central peak of the combined filter is the product of the rolloff of the individual filters, and this effect is most pronounced if both filters have about the same FWHM. Taking into account that K_1 and K_2 must be relatively prime, it would thus appear that it is best to have K_2 equal to $K_1 + 1$. The following subsection elaborates further on this point.

6.2 Ratio Optimization for Worst-Case Crosstalk

Our methodology to optimize K_1 and K_2 is similar to that used in Section 5.2, since it can be shown that that the worst case crosstalk is sensitive to the exact value of M, as was the case for the two stage filter. So, as in that case, we choose them to minimize the worst case crosstalk when M is in the vicinity of a nominal design point. In Appendix C we show that, assuming all users have unit peak power and both filters have the same finesse, the crosstalk does not exceed

$$S_V(M,F) = M(\frac{1-R}{1+R})^2 \frac{1}{(1-R^{M/K_1})} \frac{1}{(1-R^{M/K_2})}(\alpha+\beta) - 1 \tag{27}$$

where

$$\alpha = \frac{(1-R^{M/K_1+M/K_2})(1+R^{K_2+K_1})}{(1-R^{K_2+K_1})}$$

and

$$\beta = \frac{(R^{K_2}+R^{K_1})(R^{M/K_2}-R^{M/K_1})}{(R^{K_1}-R^{K_2})}$$

This bound is exact when both K_1 and K_2 divide M. The symmetry in K_1 and K_2 shows that our intuition in choosing $K_2 = K_1 + 1$ is justified. In fact the previous formula is

smooth in K_1 and K_2 and its value when $K_2 = K_1+1$ is close to that when $K_1 = K_2$ (i.e. the formula does not take into account that if K_1 actually equals K_2 then the crosstalk would dramatically increase). Further progress can be achieved by assuming that $K_1 = K_2 = K$, and due to the competing factors in the denominator K should be of the order of $\sqrt{M}$, say $K = k\sqrt{M}$. Using (5), we can rewrite (27) as

$$S_V(M,F) = \frac{\pi M}{4F^2} \frac{1}{(1-e^{-\pi k\sqrt{M}/F})^2} \left\{ \frac{(1-e^{-2\pi k\sqrt{M}/kF})(1+e^{-2\pi k\sqrt{M}/F})}{(1-e^{-2\pi k\sqrt{M}/F})} + \frac{2}{k^2} e^{-\pi\sqrt{M}/kF} \right\} - 1 \tag{28}$$

Using (28), the zero-error upperbound on M can be found to be (using $k = 0.6$):

$$M < 0.7F^2$$

Fig. 13 displays the values of K_1 minimizing (27), using $K_2 = K_1 + 1$. The ripple is due to the integer constraint. The same figure also displays the value of K minimizing (28) without the integer constraint. It can be shown that $K/\sqrt{M}$ converges to $\sqrt{1/2}$ for large M/F. The resulting values of the worst-case crosstalk are shown in Fig. 14. It should be noted that the exact and approximate values are so close that they cannot be separated in the figure.

6.3 Crosstalk PMF, BER and Power Penalty Calculation

Fig. 18 shows the crosstalk pmf when a vernier-type filter is used with $F = 100, M = 1210, K = 22$. As can be noted, the crosstalk pmf in this case appears to be more "Gaussian-like", reflecting the addition of a large number of *comparable* interference terms because the influence of the adjacent channels has been much reduced. This is not a worst-case pmf however, since M is divisible by K_1 but not by K_2.

Fig. 19 shows the resulting BER in the case of $F = 100, K = K_1 = \sqrt{0.4M}$, for different values of M such that K_1 (but not necessarily K_2, since few such pairs exist) divides M. As can be easily seen, the BER degradation due to crosstalk is significantly smaller than in the case of the two-stage filter. In addition, the power penalty is observed to be significantly smaller, for equal values of M, than in the previous cases, as shown in Fig. 20.

7 Discussion and Conclusions

We have investigated in this paper the performance of four different Fabry-Perot filter structures that may be used as filters or demultiplexers in wavelength division multiplexed networks. The criteria uses for performance comparison were the resulting worst-case crosstalk, BER and crosstalk power penalty. The double-cavity structures all outperformed the single cavity structure, with the optimized vernier-type filter producing the best performance.

As a specific example, consider the case when the maximum allowed crosstalk-induced penalty is 1 dB at a BER of 10^{-9}. Table 1 shows the maximum number of users M that is allowed with F values of 100 and 300. As can be seen, the difference between the performance of the Vernier filter and the two-stage filter is much greater than that of both the double-pass and the single-cavity filters.

It is necessary to add here though that while the vernier type double-cavity filter may perform best, it is probably also the most difficult to implement since keeping the ratio of the free spectral ranges constant over the entire tuning range is likely to be a complex and delicate operation. Thus a suitable alternative is the two-stage filter, which is easier to control, but at the expense of some performance loss.

Finally, it must be emphasized that the systems analyzed in this paper were highly idealistic, since several important practical limitations, such as the stability of both the lasers and the filters, finite laser linewidths, and filter tunability were not taken into account. Many of these phenomena will become dominant when M is large. For example, if 10^4 users are placed in the low-loss window of 1.5-1.6 microns, this will result in channel separations of approximately 1 Ghz, so that the above phenomena may be the main causes of degradation, and our results may no longer reflect the truly attainable performance. Further research is thus necessary to determine the full effect of these limitations on Fabry-Perot filter-based dense WDM systems.

8 Acknowledgments

We wish to thank Paul Green for his continuing encouragement and support. Further thanks go to Karen Liu, Rajiv Ramaswami, Frank Tong and all other members of the Advanced Optical Networking group at IBM for many fruitful discussions.

A Appendix

We derive the total power T transmitted through a lossless FP filter with mirror reflectivities R, by M unit power users equally spaced in frequency over the free spectral range of the filter, with a normalized frequency offset Δ with respect to a peak transmission frequency.

It is convenient here to use the alternate form of the transfer function (3), which is simply the Fourier series expansion of the Airy function (4). We then have

$$T = \frac{1-R}{1+R} \sum_{i=0}^{M-1} \sum_{n=-\infty}^{\infty} R^{|n|} e^{j2\pi n(\Delta + \frac{i}{M})} \tag{A.1}$$

$$= \frac{1-R}{1+R} \sum_{n=-\infty}^{\infty} R^{|n|} \sum_{i=0}^{M-1} e^{j2\pi n(\Delta + \frac{i}{M})} \tag{A.2}$$

But

$$\sum_{i=0}^{M-1} e^{\frac{j2\pi in}{M}} = \begin{cases} M & n = mM \quad , m \text{ integer} \\ 0 & \text{otherwise} \end{cases} \tag{A.3}$$

Thus,

$$T = M \frac{1-R}{1+R} \sum_{m=-\infty}^{\infty} R^{M|m|} e^{j2\pi \Delta m M} \tag{A.4}$$

Comparing (A.4) with (3), we recognize that the last sum is proportional to the power transmitted by a single user with a normalized frequency offset $M\Delta$ through a FP filter with mirror reflectivity R^M. Simplifying,

$$T = M\left(\frac{1-R}{1+R}\right)\left(\frac{1+R^M}{1-R^M}\right) \frac{1}{1 + ((2\sqrt{R^M}/(1-R^M))sin(\pi M \Delta))^2} \tag{A.5}$$

Substituting $\Delta = 0$, and subtracting 1 (the desired signal) we get (9).

B Appendix

The following inequalities hold for $x \geq 0$

$$\frac{x^2}{6+x} \leq \frac{x(e^x+1)}{e^x-1} - 2 \leq \frac{x^2}{6}$$

Proof: Consider the function

$$f(x) = \frac{x(e^x+1)}{e^x-1} - 2 - \frac{x^2}{6+bx} \tag{B.1}$$

$$= \frac{e^x(x^2(b-1)+x(6-2b)-12)+x^2(1+b)+x(6+2b)+12}{(e^x-1)(6+bx)} \tag{B.2}$$

where b is a parameter. For x and b non-negative, the function has the same sign as the numerator. The first three derivatives of the numerator are

$$\begin{aligned} f'(x) &= e^x(x^2(b-1)+4x-6-2b)+x(2+2b)+6+2b \\ f''(x) &= e^x(x^2(b-1)+x(2+2b)-2-2b)+2(1+b) \\ f'''(x) &= e^x(x^2(b-1)+4xb) \end{aligned}$$

One sees that the numerator itself and its first two derivatives are 0 at $x = 0$, but that the third derivative is non-positive for $b = 0$, and non-negative for $b = 1$ and $x \geq 0$. This proves the desired inequalities.

C Appendix

We derive here a tight upperbound on the total power T transmitted through two independent lossless FP filters by M unit power users equally spaced in frequency. We assume that the system bandwidth is K_1 and K_2 times the free spectral range of filters 1 and 2 respectively, and that the frequency of one user coincides with transmission peaks of both filters. K_1 and K_2 are assumed to be relatively prime integers so that this double coincidence occurs only for one user. R_1 and R_2 will denote the mirror reflectivities of filters 1 and 2 respectively.

From (3) we have,

$$T = M\frac{1-R_1}{1+R_1}\frac{1-R_2}{1+R_2}\sum_{i=0}^{M-1}\sum_{n_1=-\infty}^{\infty}\sum_{n_2=-\infty}^{\infty} R_1^{|n_1|}R_2^{|n_2|}e^{j2\pi i(\frac{n_1K_1+n_2K_2}{M})} \tag{C.1}$$

Using (A.3), only the values of n_1 and n_2 such that

$$\frac{n_1K_1+n_2K_2}{M} = l \tag{C.2}$$

for l integer, will contribute to the sum.

As K_1 and K_2 are relatively prime, Euclid's Greatest Common Divisor algorithm guarantees that there exists integers N_1 and N_2 such that $N_1K_1 - N_2K_2 = 1$. Thus (C.2) can be rewritten as

$$K_1(n_1 - N_1lM) + K_2(n_2 + N_2lM) = 0$$

It follows that $n_1 - N_1lM$ is 0 modulo K_2, and $n_2 + N_2lM$ is 0 modulo K_1. The n_1 and n_2 that satisfy (C.2) must have the form $n_1 = lN_1M + jK_2$ and $n_2 = -(lN_2M + jK_1)$ for some integer j.

We can thus rewrite (C.1) as

$$T = M\frac{1-R_1}{1+R_1}\frac{1-R_2}{1+R_2}\sum_{l=-\infty}^{\infty}\sum_{j=-\infty}^{\infty} R_1^{|lN_1M+jK_2|}R_2^{|lN_2M+jK_1|} \tag{C.3}$$

Fig. 21 plots $|n_1|$ and $|n_2|$ versus j for a given l. It shows that there is a point n_1' where $|n_1|$ is less than K_2 on one side of the central region, and a point n_2' where $|n_2|$ is less than K_1 on the other side. We denote the corresponding values of $|n_2|$ and $|n_1|$ for the same j's by n_2'' and n_1'' respectively. Note that n_1', n_2', n_1'', n_2'' all implicitly depend on l. One sees from (C.2) that

$$n_2'' = |l|\frac{M}{K_2} + n_1'\frac{K_1}{K_2} \tag{C.4}$$

and similarly for n_1''. With these auxiliary definitions, it is simple to find an expression for the sum over j in (C.3), as it decomposes into power series in the central and side regions of Fig. 21. We obtain

$$T = M\frac{1-R_1}{1+R_1}\frac{1-R_2}{1+R_2}\sum_{l=-\infty}^{\infty} A_l \tag{C.5}$$

where

$$A_l = \frac{R_1^{n_1'}R_2^{n_2''} + R_1^{n_1''}R_2^{n_2'}}{1-R_1^{K_2}R_2^{K_1}} + \frac{R_1^{K_2-n_1'}R_2^{n_2''} - R_1^{n_1''}R_2^{K_1-n_2'}}{R_2^{K_1}-R_1^{K_2}} \tag{C.6}$$

Consider now n_1' and n_2' in (C.6) as independent variables and n_1'' and n_2'' as variables that depend on l, n_1' and n_2' through (C.4). Using that formula, the part of A_l that depends on n_1' (first and third terms) can be written as

$$R_2^{|l|M/K_2}\left(\frac{(R_1^{K_2}R_2^{K_1})^{n_1'/K_2}}{1-R_1^{K_2}R_2^{K_1}} - \frac{(R_2^{K_1}/R_1^{K_2})^{n_1'/K_2}}{1-R_2^{K_1}/R_1^{K_2}}\right) \tag{C.7}$$

The value of this expression is the same for $n_1' = 0$ and $n_1' = K_2$. Moreover the difference between the value at $n_1' = 0$ and the general expression is

$$R_2^{|l|M/K_2}\left(\frac{1-(R_1^{K_2}R_2^{K_1})^{n_1'/K_2}}{1-R_1^{K_2}R_2^{K_1}} - \frac{1-(R_2^{K_1}/R_1^{K_2})^{n_1'/K_2}}{1-R_2^{K_1}/R_1^{K_2}}\right)$$

One verifies that this quantity is positive if $0 < n_1'/K_2 < 1$ because $R_2^{K_1}/R_1^{K_2}$ exceeds $R_1^{K_2}R_2^{K_1}$, and the function $(1-x^\alpha)/(1-x)$ decreases with $x > 0$ for $0 < \alpha < 1$. Thus the maximum of (C.7) occurs at $n_1' = 0$. The same reasoning holds for n_2'. We can thus obtain an upper bound for A_l by using $n_1' = n_2' = 0$, and from (C.2), $n_1'' = |l|M/K_1$ and $n_2'' = |l|M/K_2$, yielding

$$A_l \leq \frac{R_2^{|l|M/K_2} + R_1^{|l|M/K_1}}{1-R_1^{K_2}R_2^{K_1}} + \frac{R_1^{K_2}R_2^{|l|M/K_2} - R_1^{|l|M/K_1}R_2^{K_1}}{R_2^{K_1}-R_1^{K_2}} \tag{C.8}$$

Summing over l gives the following bound on T:

$$T \leq M\frac{1-R_1}{1+R_1}\frac{1-R_2}{1+R_2}\frac{1}{(1-R_1^{M/K_1})}\frac{1}{(1-R_2^{M/K_2})}[\alpha+\beta] \tag{C.9}$$

where

$$\alpha = \frac{(1 - R_1^{M/K_1} R_2^{M/K_2})(1 + R_1^{K_2} R_2^{K_1})}{(1 - R_1^{K_2} R_2^{K_1})}$$

and

$$\beta = \frac{(R_1^{K_2} + R_2^{K_1})(R_2^{M/K_2} - R_1^{M/K_1})}{(R_2^{K_1} - R_1^{K_2})}]$$

β above is always positive and simplifies to $\frac{2M}{K_1 K_2} R_1^{M/K_1}$ when $R_2^{K_1} = R_1^{K_2}$.

This bound is achieved with equality when M is such that n_1' and n_2' are zero for all l, which occurs when K_1 and K_2 both divide M. In that case there is a transmitter frequency at each peak of the series transmission of the filter.

By substituting $R_1 = R_2 = R, K_1 = 1, K_2 = M$, and subtracting 1 we get (9). If we substitute as above but with $K_2 = 1$, we get (17).

D References

[1] J. Stone and L. W. Stulz, "Pigtailed High-finesse tunable fiber Fabry-Perot interferometers with large, medium and small free spectral ranges", *Electronics Letters*, vol. 23, pp. 781-783, 1987.

[2] J. Stone and D. Marcuse, "Ultrahigh finesse fiber Fabry-Perot interferometers", *J. Lightwave Technol.*, vol. LT-4, pp. 382-385, 1986.

[3] I. P. Kaminow, P. P. Iannone, J. Stone and L. W. Stulz, "FDMA-FSK Star network with a tunable optical filter demultiplexer", *J. Lightwave Technol.*, vol. LT-6, pp. 1406-1414, 1988.

[4] A. A. M. Saleh and J. Stone, "Two-stage Fabry-Perot filters as demultiplexers in optical FDMA LAN's", *J. Lightwave Technol.*, vol. LT-7, pp. 323-330, 1989.

[5] A. R. Chraplyvy, R. W. Tkach, and R. M. Derosier, "Network experiment using an 8000 GHz tuning range optical filter", *Electronic Letters*, vol. 24, pp. 1071-1072, 1988.

[6] A. Frenkel and C. Lin. "Angle-tuned etalon filters for optical channel selection in high density wavelength division multiplexed systems", *J. Lightwave Technol.*, vol. LT-7, pp. 615-624, 1989.

[7] S. R. Mallinson, "Wavelength selective filters for single-mode fiber WDM systems using Fabry-Perot Interferometers", *Appl. Opt.*, vol. 26, pp. 430-436, 1987.

[8] S. R. Mallinson, "Crosstalk limits of Fabry-Perot demultiplexers", *Electronics Letters*, vol. 21, pp. 759-760, 1985.

[9] A. M. Hill and D. B. Payne, "Linear crosstalk in wavelength division multiplexed optical fiber transmission systems", *J. Lightwave Technol.*, vol. LT-3, pp. 643-651, 1985.

[10] B. L. Kasper, "Receiver Design", in *Optical Fiber Telecommunications II*, S. E. Miller and I. P. Kaminow ed., Academic Press, 1988.

[11] G. Hernandez, *Fabry-Perot Interferometers*, Cambridge University Press, 1986.

[12] H. van de Stadt and J. M. Muller, "Multimirror Fabry-Perot interferometers", *J. Opt. Soc. Am A*, vol. 2, pp. 1363-1370, 1985.

List of Figure Captions

Fig. 1: Illustrative diagram of the four Fabry-Perot structures analyzed in the paper.

Fig. 2: Comparison of the transfer functions of the four FP structures, for the cases: Single Cavity finesse $F = 100$, $K = 10$, $K_1 = K_2 - 1 = 6$.

Fig. 3: (a) Crosstalk probability mass function (pmf) for the Single-Cavity FP filter ($M = 40$, $F = 100$). (b) Crosstalk pmf for ZERO and ONE levels for ($M = 80$, $F = 100$). Threshold value is shown.

Fig. 4: Worst-case crosstalk for Single-Cavity and Double-Pass FP filters ($F = 100$) versus M, and approximations to them. Note only two curves appear due to the excellence of the approximations.

Fig. 5: BER versus SNR for different values of M/F, $F = 100$, for the Single-Cavity FP filter.

Fig. 6: Crosstalk power penalty for 4 different BERs for the Single-Cavity filter.

Fig. 7: BER versus SNR for different values of worst-case laser drift (normalized by FWHM).

Fig. 8: Normalized optimum finesse F^* and optimum crosstalk power penalty versus normalized M. Normalization factor is A^{-1} where A is the loss parameter of both mirrors.

Fig. 9: Crosstalk pmf for Double-Pass FP filter. $M = 112$, $F = 100$, $S_{DP}(M, F)$ defined in (18).

Fig. 10: BER versus SNR for different values of M/F, $F = 100$, for the Double-Pass FP filter.

Fig. 11: Crosstalk power penalty versus M/F for different BERs for Double-Pass FP filter.

Fig. 12: Variation of worst-case crosstalk for Two-Stage FP filter versus M. $F = 100$, $K = 28$. Bound (22) is also plotted.

Fig. 13: Variation of optimum K with M, $F = 100$, for Two-Stage and Vernier FP filters ($K_1 = K$).

Fig. 14: Optimum worst-case crosstalk for Two-Stage and Vernier filters. Exact and approximate formulas are plotted for both filters, (which overlap for the Vernier case).

Fig. 15: Crosstalk pmf for Two-Stage FP filter for two cases: $M = 784, F = 100, K = 28$ and $M = 800, F = 100, K = 28$. Note $S_{TS}(M, F, K)$ is larger for the first case (M smaller) since 28 divides 784 and is thus a worst-case.

Fig. 16: BER versus SNR for different $M, F = 100, K = \sqrt{M}$ for the Two-Stage FP filter.

Fig. 17: Crosstalk power penalty versus M/F^2 for different BERs for the Two-Stage FP filter, for $F = 100$.

Fig. 18: Crosstalk pmf for Vernier filter, with $M = 1210, F = 100, K_1 = 22$.

Fig. 19: BER versus SNR for different values of $M, F = 100, K = \sqrt{0.4M}$ for the Vernier FP filter.

Fig. 20: Crosstalk power penalty versus M/F^2 for different BERs for the Vernier FP filter, for $F = 100$.

Table 1: Performance comparison of the four FP structures for a 1 dB crosstalk power penalty. See comments in Section 7.

Fig. 21: Diagram illustrating relationship between n_1', n_2', n_1'', n_2'', and K_1, K_2.

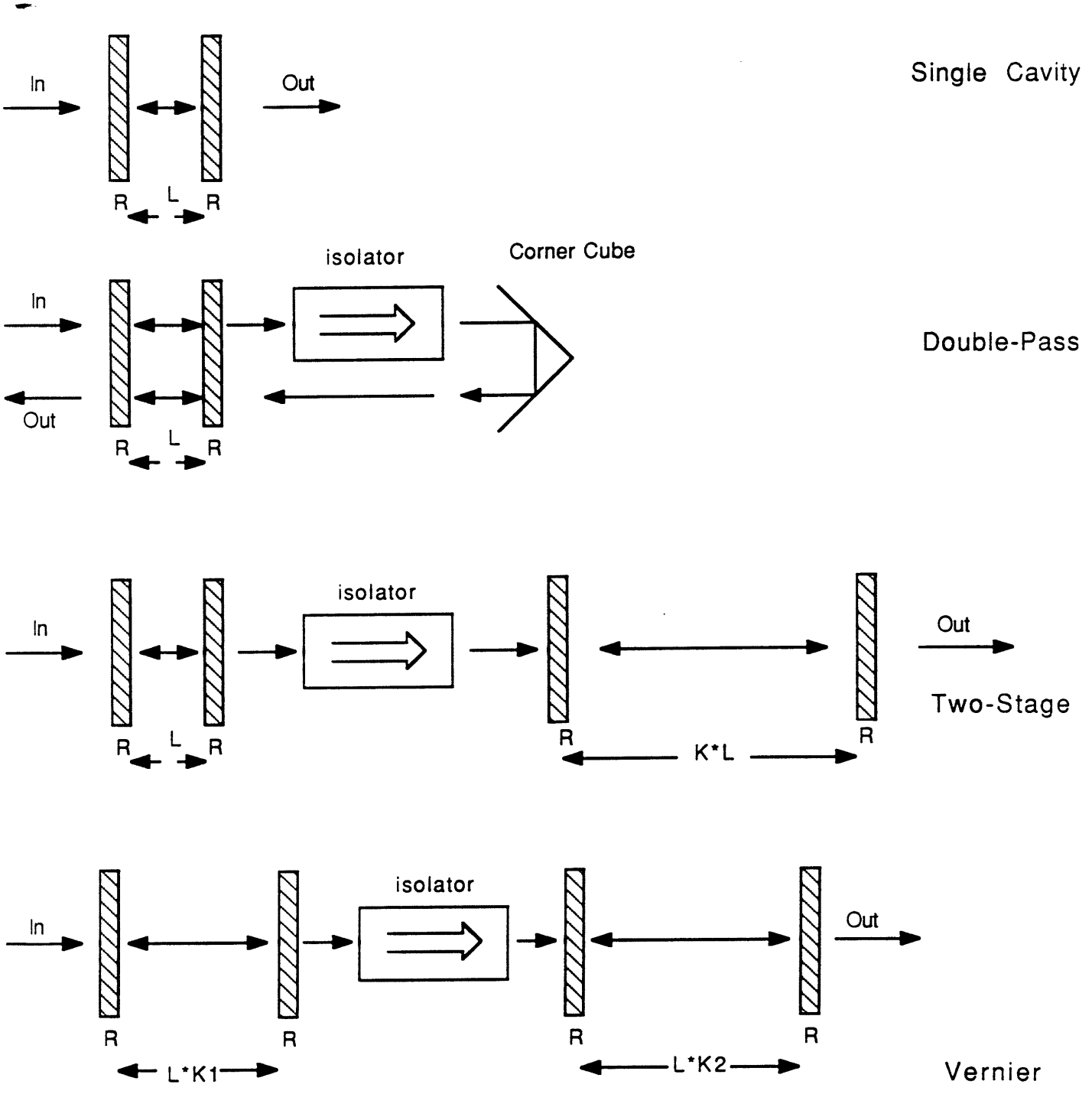
In
Out
R
L
R
Single Cavity
isolator
Corner Cube
In
Out
R
L
R
Double-Pass
In
isolator
R
L
R
R
K*L
R
Out
Two-Stage
In
isolator
R
R
L*K1
R
R
L*K2
Out
Vernier

Fig 1

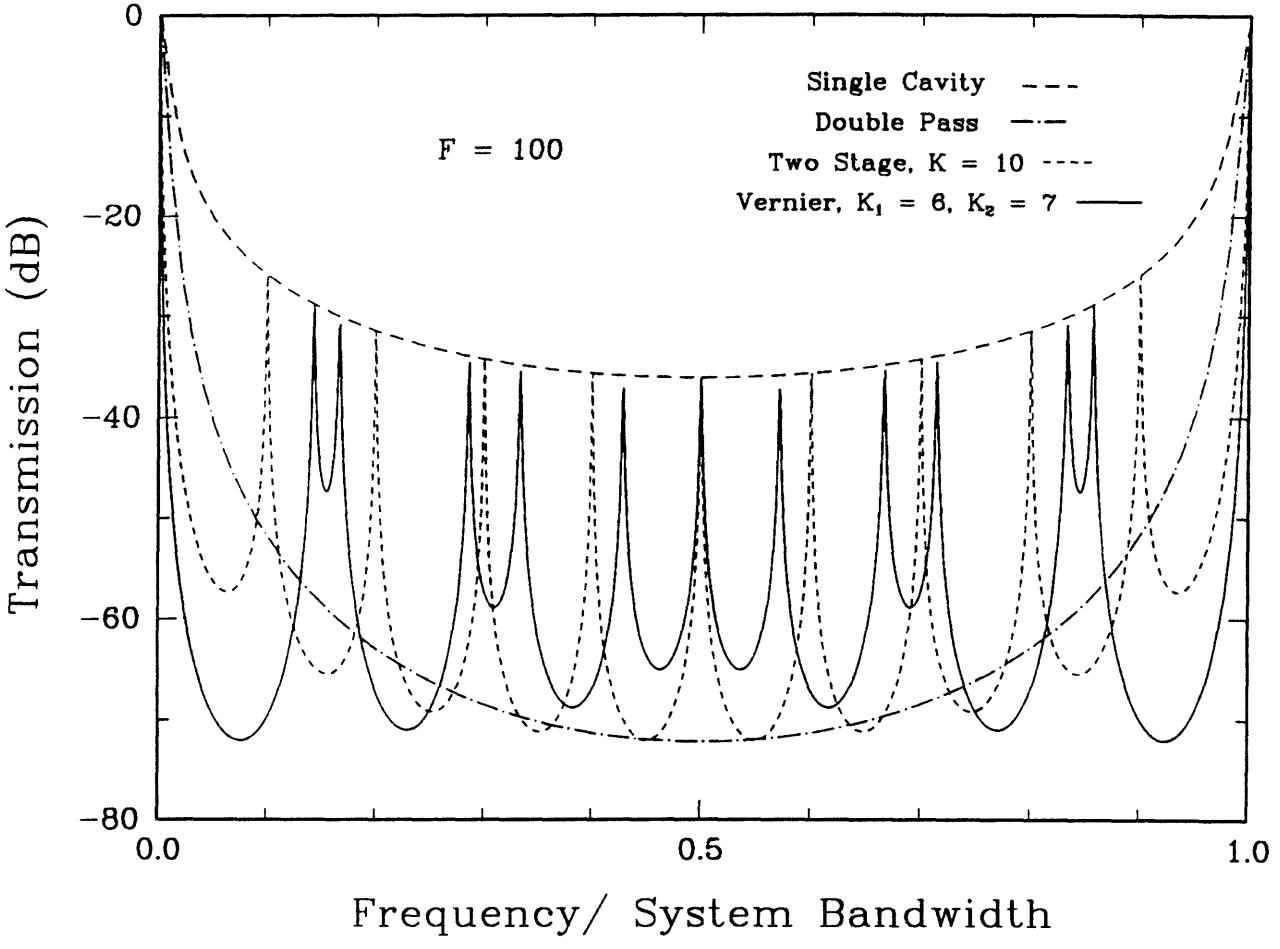
0
-20
-40
-60
-80
0.0
0.5
1.0
Transmission (dB)
Frequency/ System Bandwidth
F = 100
Single Cavity
Double Pass
Two Stage, K = 10
Vernier, K1 = 6, K2 = 7

Fig 2

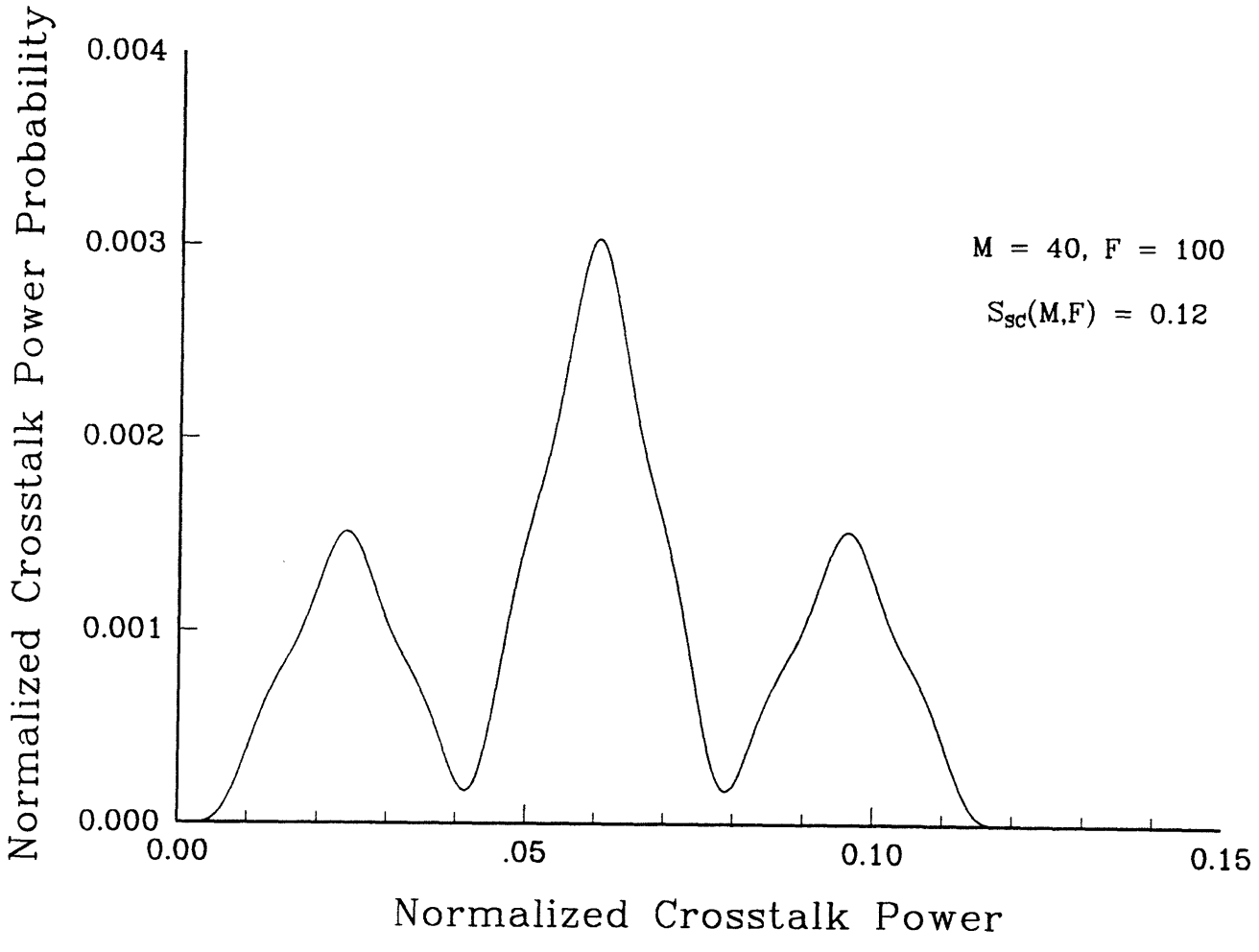
Normalized Crosstalk Power Probability
0.004
0.003
0.002
0.001
0.000
0.00
.05
0.10
0.15
Normalized Crosstalk Power
M = 40, F = 100
$S_{sc}(M,F)$ = 0.12

Fig 3(a)

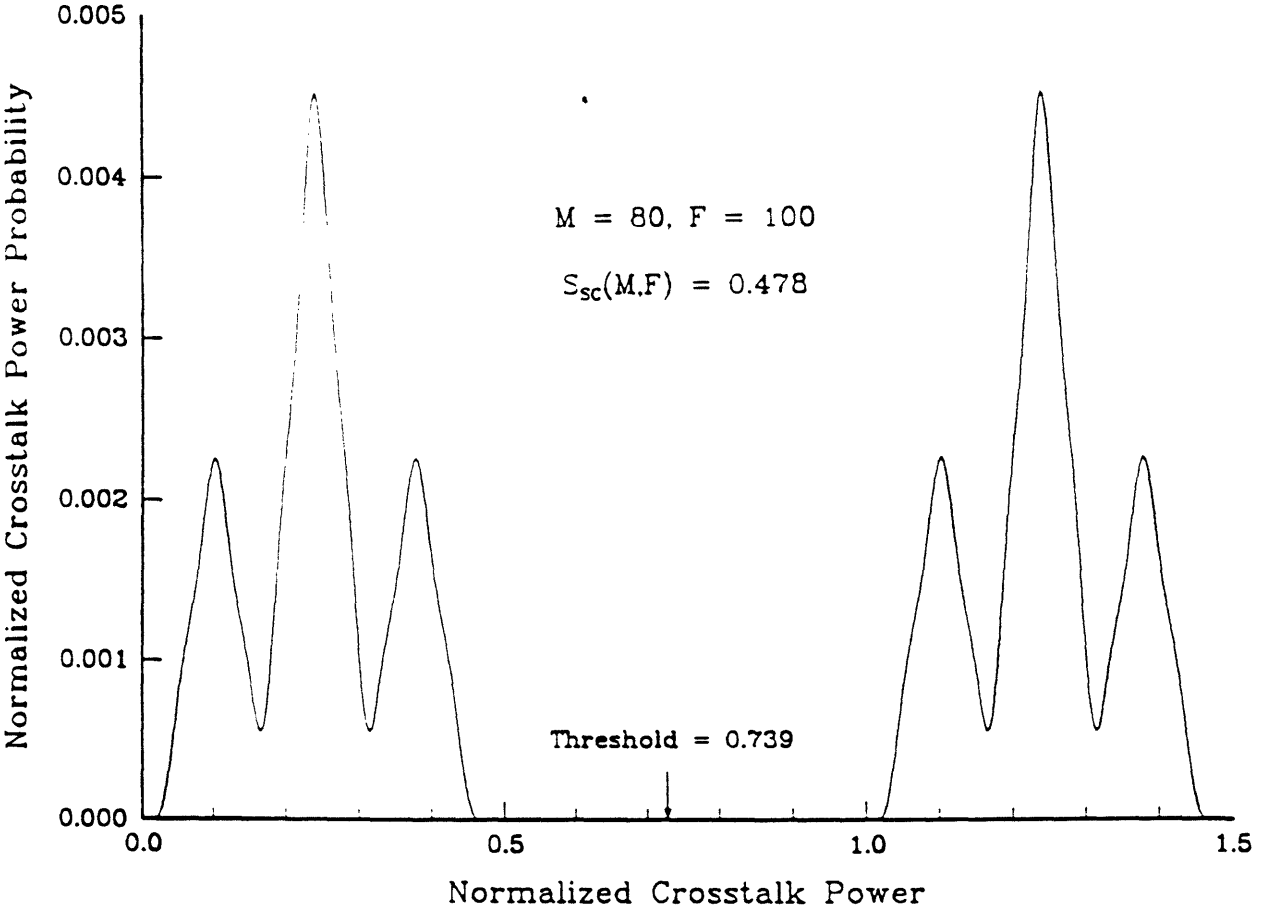
0.005
0.004
0.003
0.002
0.001
0.000
Normalized Crosstalk Power Probability
M = 80, F = 100
$S_{sc}(M,F)$ = 0.478
Threshold = 0.739
0.0
0.5
1.0
1.5
Normalized Crosstalk Power

Fig 3(b)

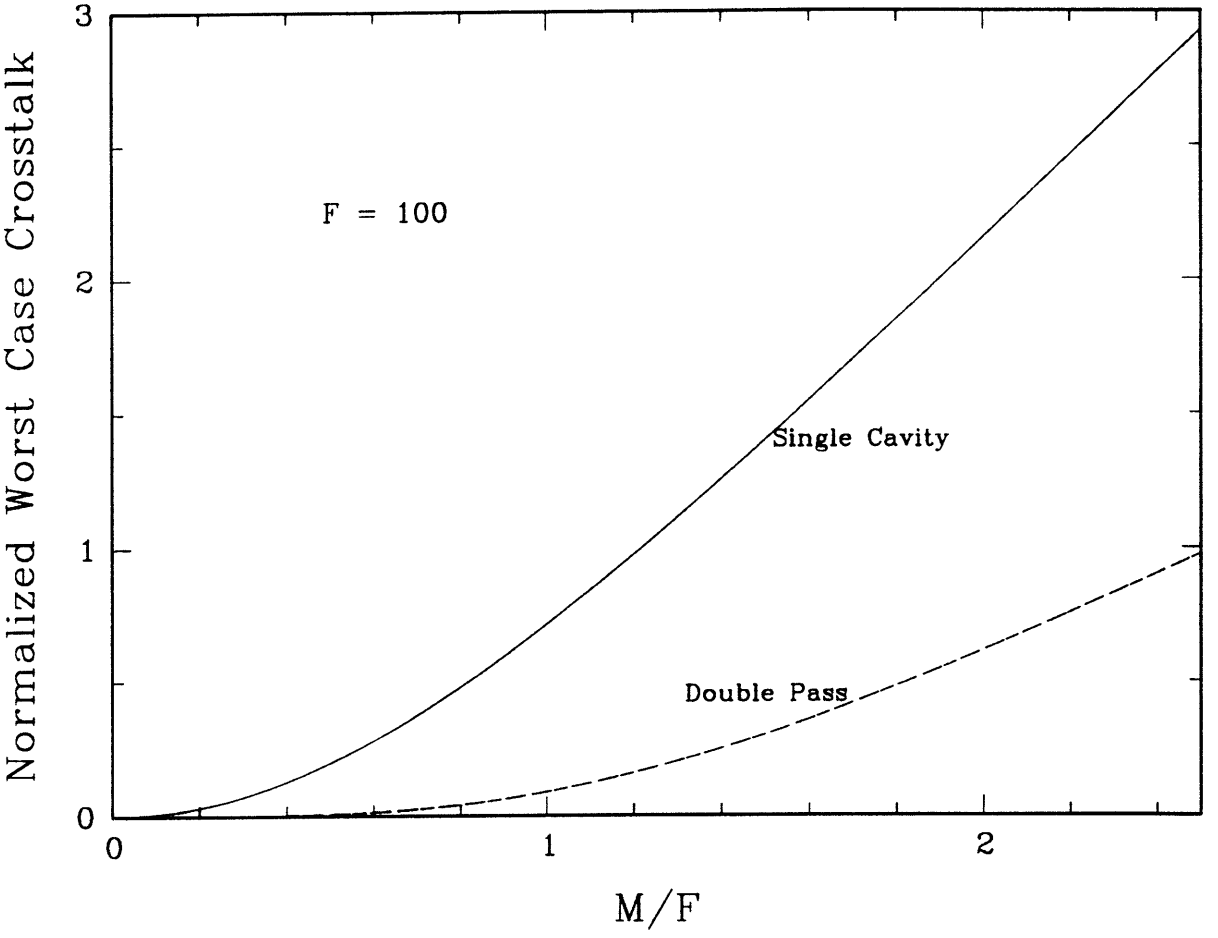
Normalized Worst Case Crosstalk
3
2
1
0
F = 100
Single Cavity
Double Pass
0
1
2
M/F

Fig 4

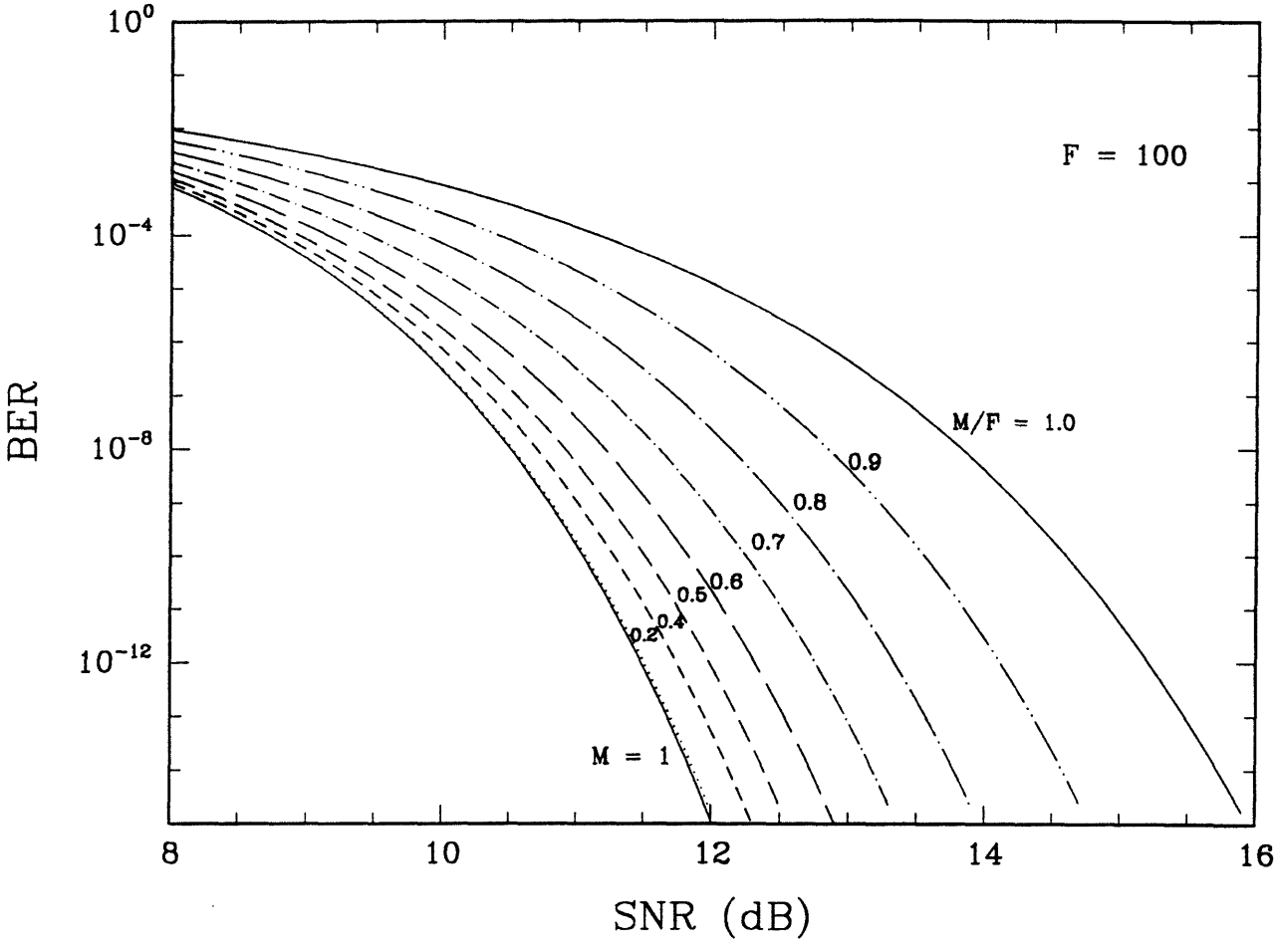
10^0
10^{-4}
10^{-8}
10^{-12}
BER
F = 100
M/F = 1.0
0.9
0.8
0.7
0.6
0.5
0.4
0.2
M = 1
8
10
12
14
16
SNR (dB)

Fig 5

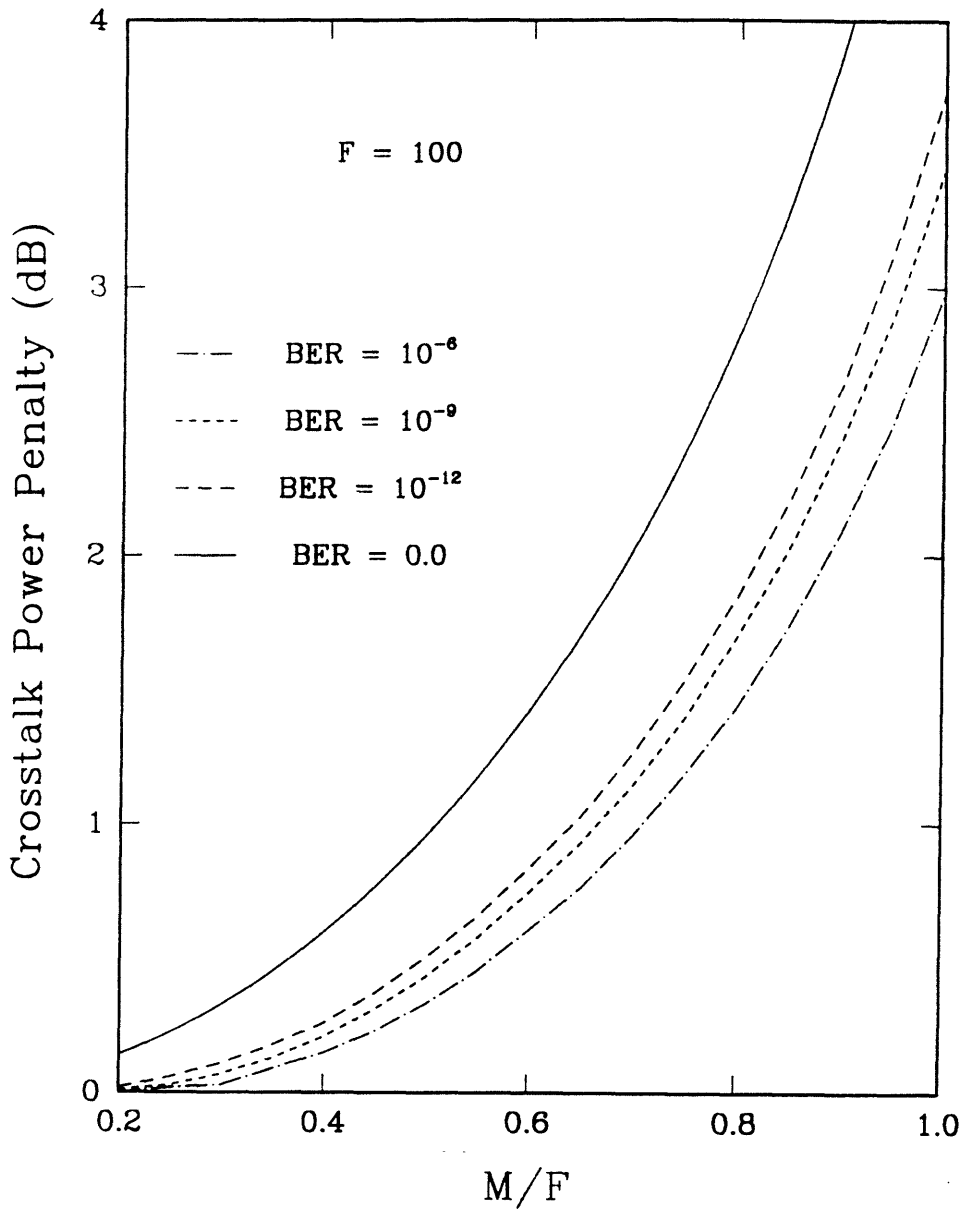
4
3
2
1
0
0.2
0.4
0.6
0.8
1.0
F = 100
BER = 10^{-6}
BER = 10^{-9}
BER = 10^{-12}
BER = 0.0
Crosstalk Power Penalty (dB)
M/F

Fig 6

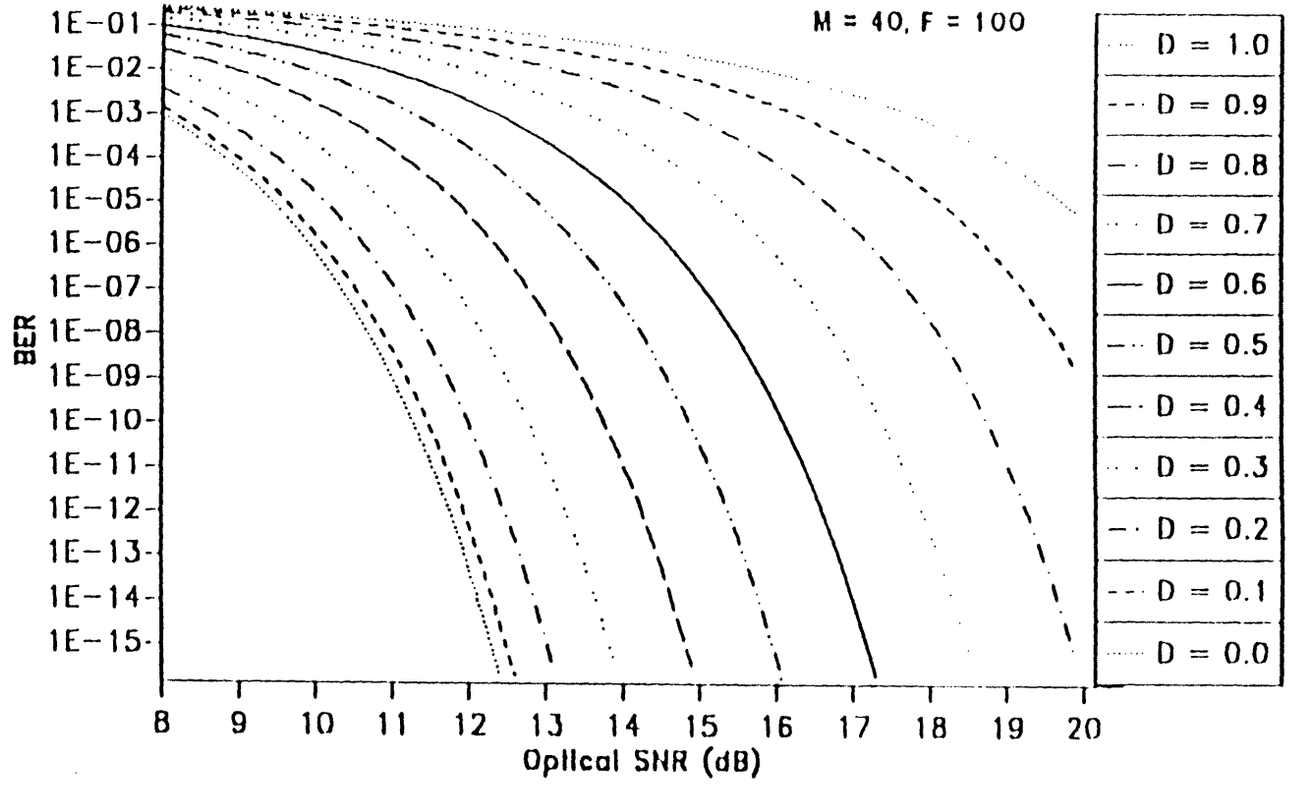
M = 40, F = 100
BER
1E-01
1E-02
1E-03
1E-04
1E-05
1E-06
1E-07
1E-08
1E-09
1E-10
1E-11
1E-12
1E-13
1E-14
1E-15
8
9
10
11
12
13
14
15
16
17
18
19
20
Optical SNR (dB)
D = 1.0
D = 0.9
D = 0.8
D = 0.7
D = 0.6
D = 0.5
D = 0.4
D = 0.3
D = 0.2
D = 0.1
D = 0.0

Fig 7

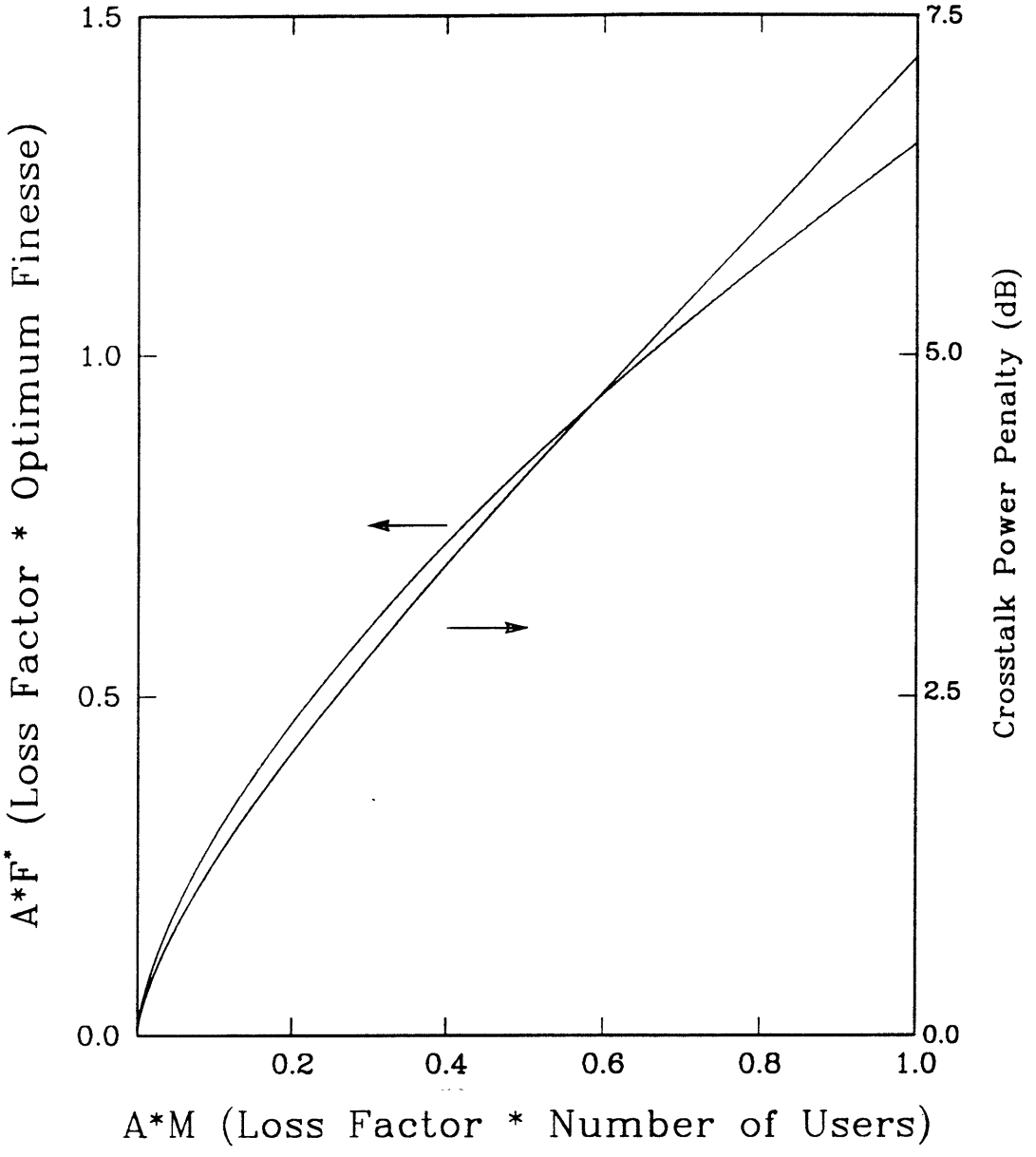
1.5
1.0
0.5
0.0
7.5
5.0
2.5
0.0
0.2
0.4
0.6
0.8
1.0
A*F* (Loss Factor * Optimum Finesse)
Crosstalk Power Penalty (dB)
A*M (Loss Factor * Number of Users)

Fig. 8

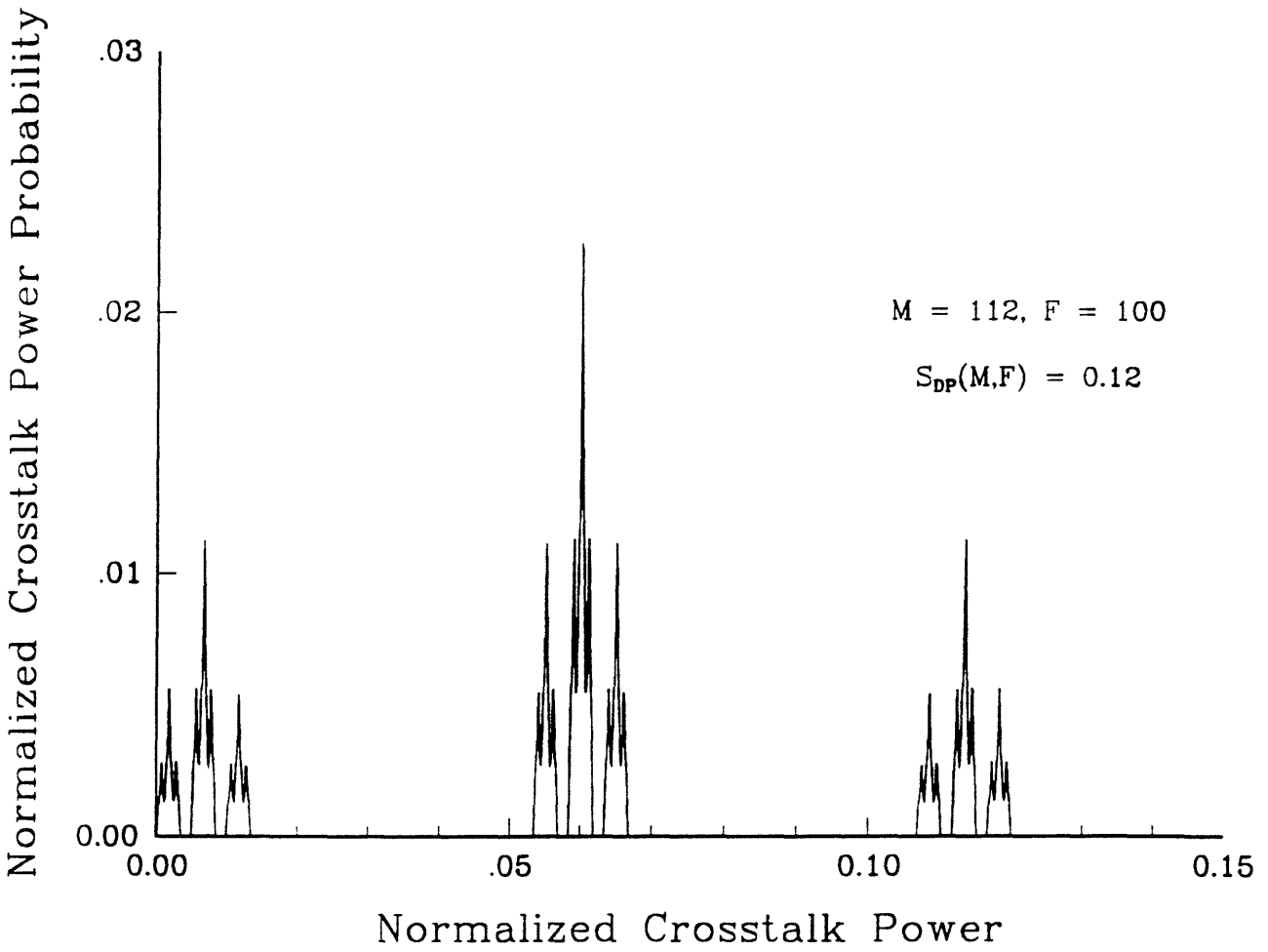
Normalized Crosstalk Power Probability
.03
.02
.01
0.00
0.00
.05
0.10
0.15
Normalized Crosstalk Power
M = 112, F = 100
$S_{DP}(M,F)$ = 0.12

Fig. 9

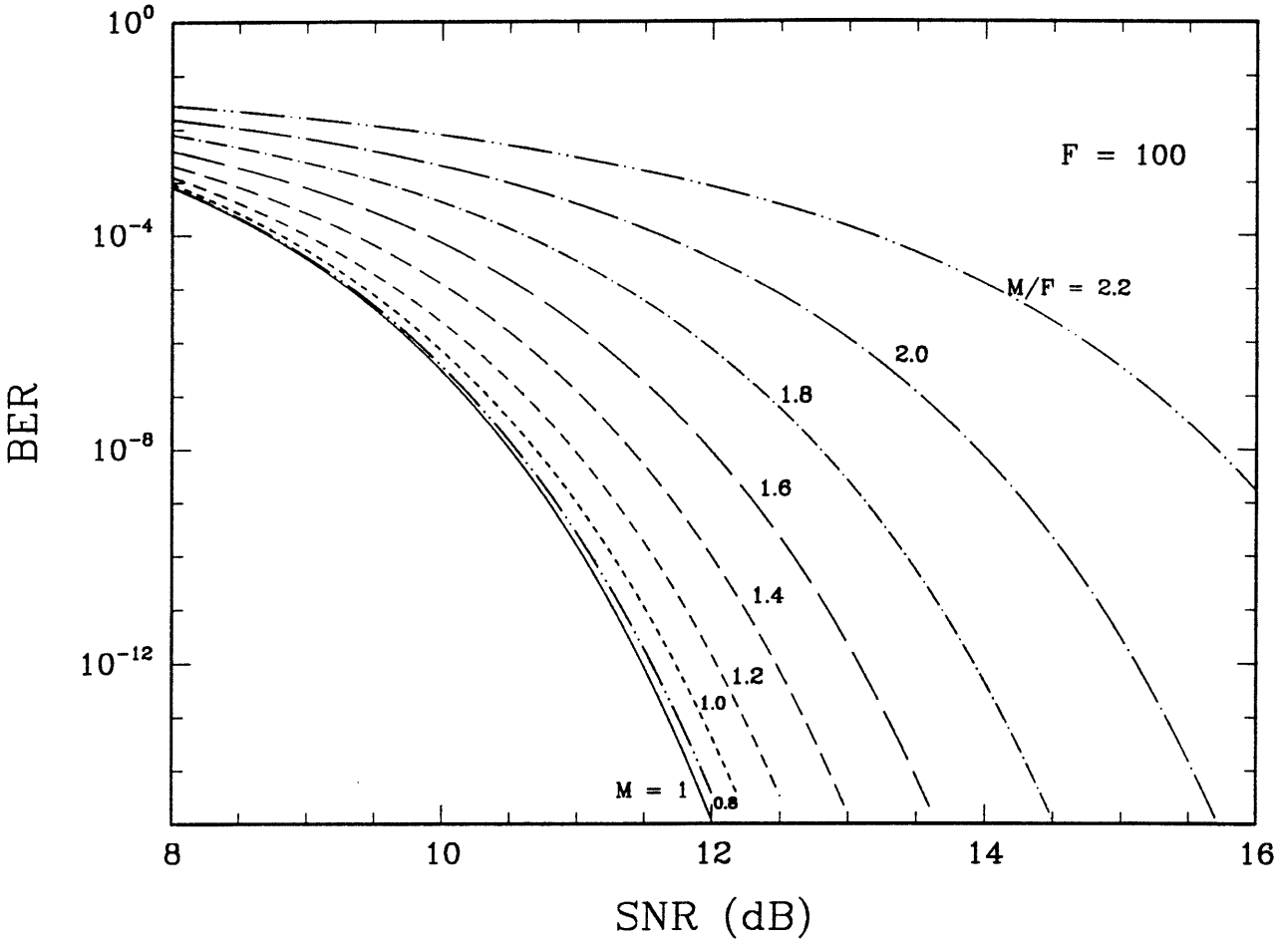
10^0
10^{-4}
10^{-8}
10^{-12}
BER
F = 100
M/F = 2.2
2.0
1.8
1.6
1.4
1.2
1.0
0.8
M = 1
8
10
12
14
16
SNR (dB)

Fig. 10

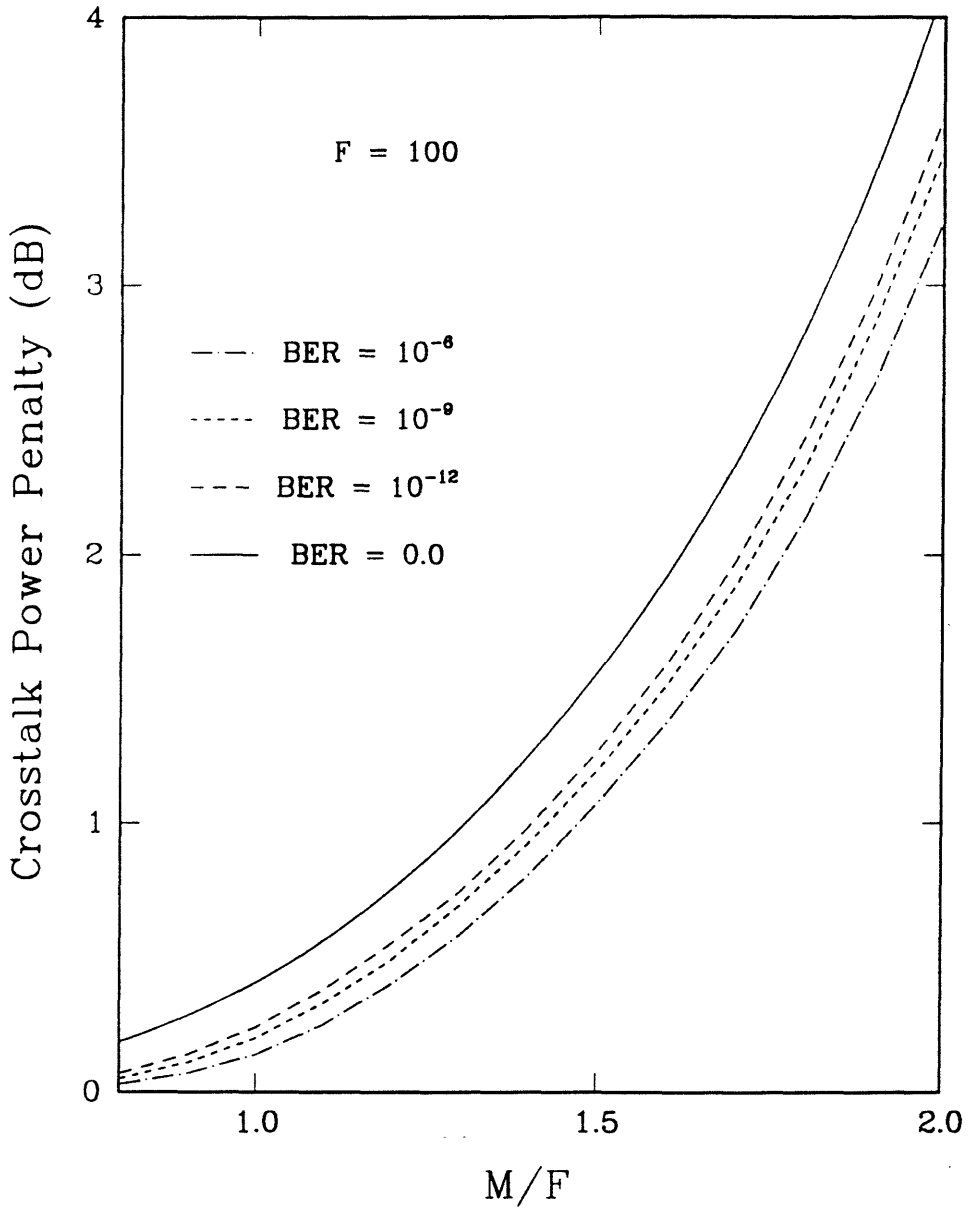
F = 100
BER = 10^{-6}
BER = 10^{-9}
BER = 10^{-12}
BER = 0.0
Crosstalk Power Penalty (dB)
0
1
2
3
4
1.0
1.5
2.0
M/F

Fig. 11

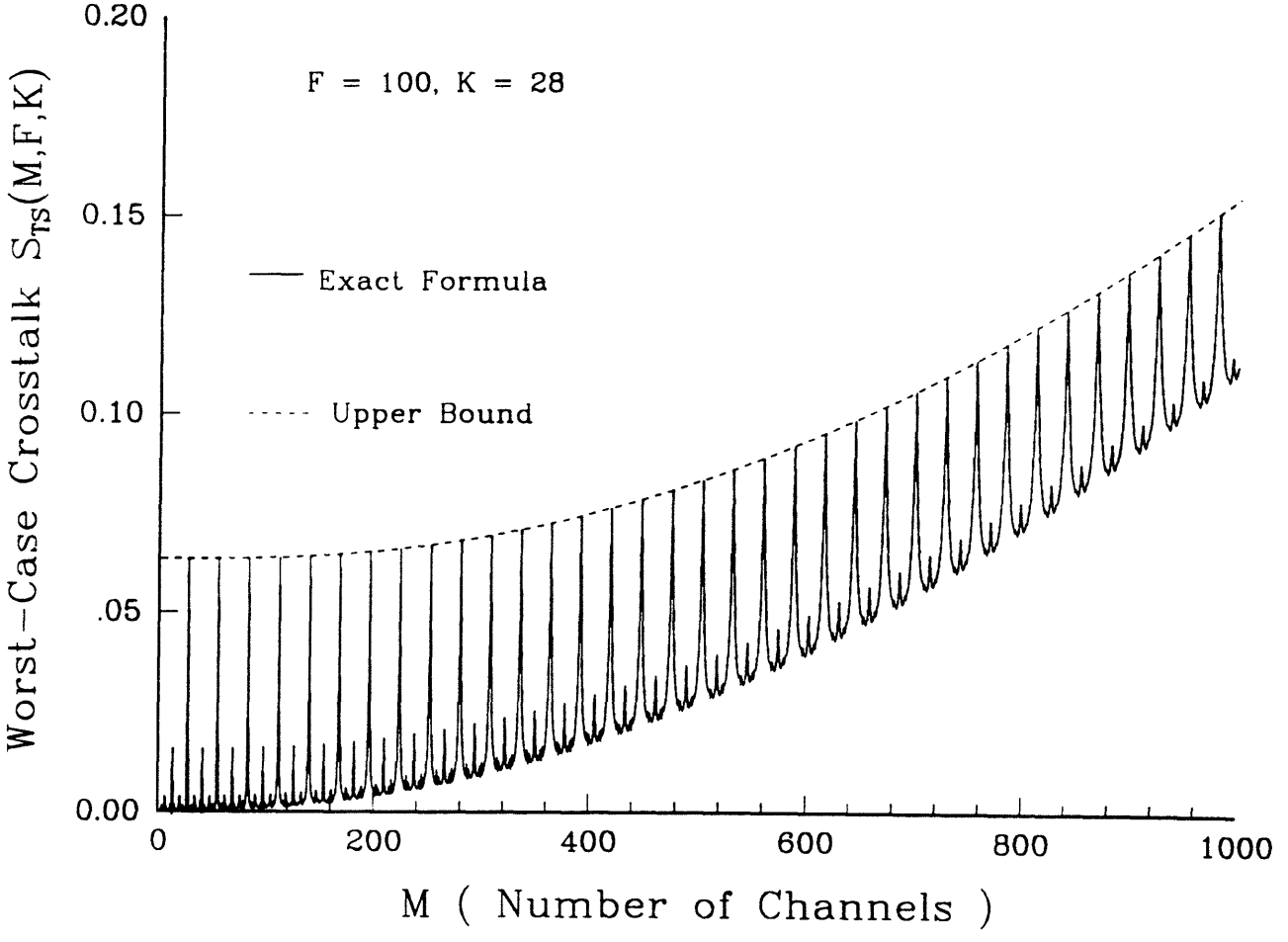
0.20
0.15
0.10
.05
0.00
F = 100, K = 28
Exact Formula
Upper Bound
Worst-Case Crosstalk $S_{TS}(M,F,K)$
0
200
400
600
800
1000
M (Number of Channels)

Fig. 12

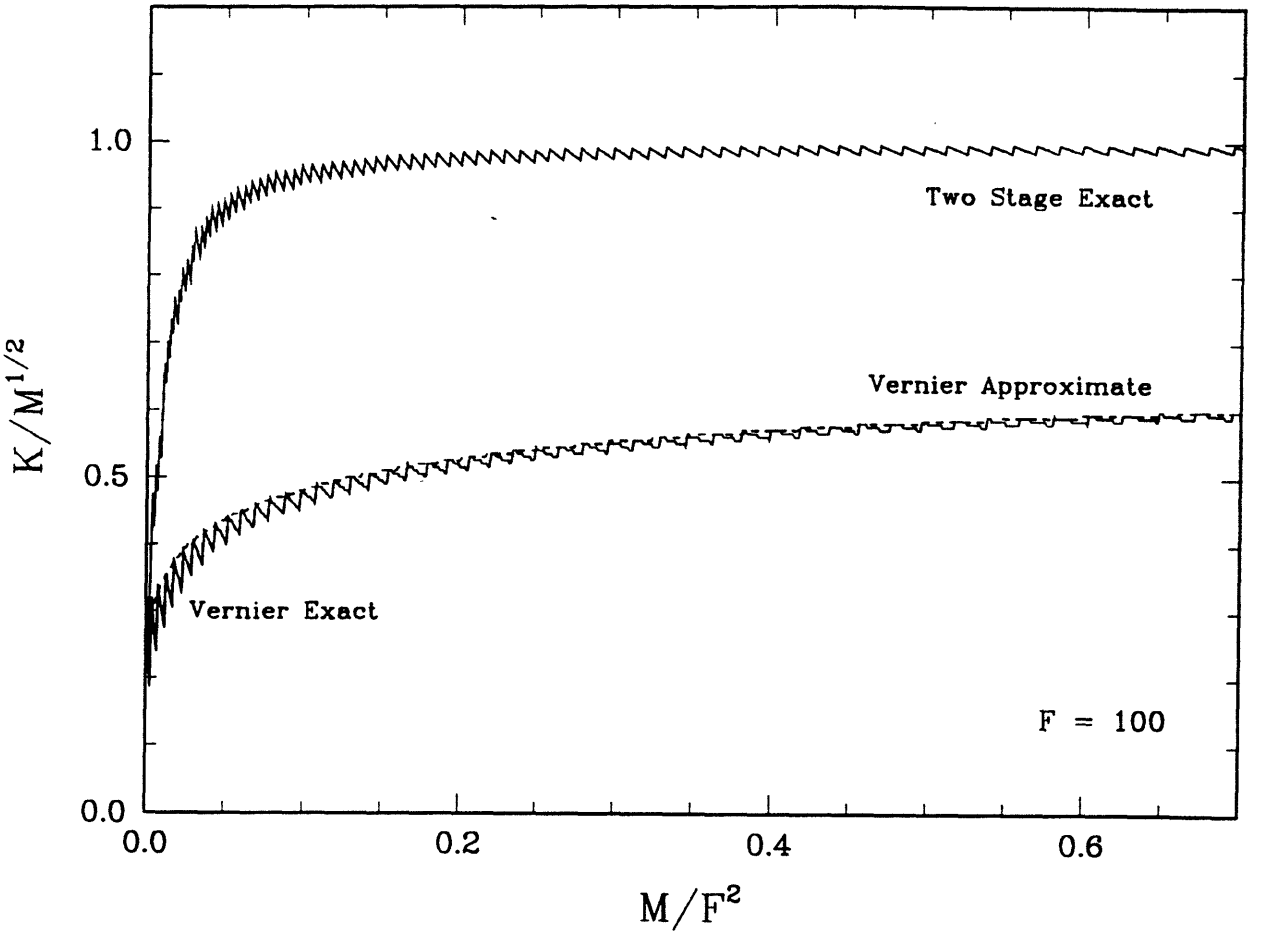
1.0
0.5
0.0
0.0
0.2
0.4
0.6
K/M^1/2
M/F^2
Two Stage Exact
Vernier Approximate
Vernier Exact
F = 100

Fig. 13

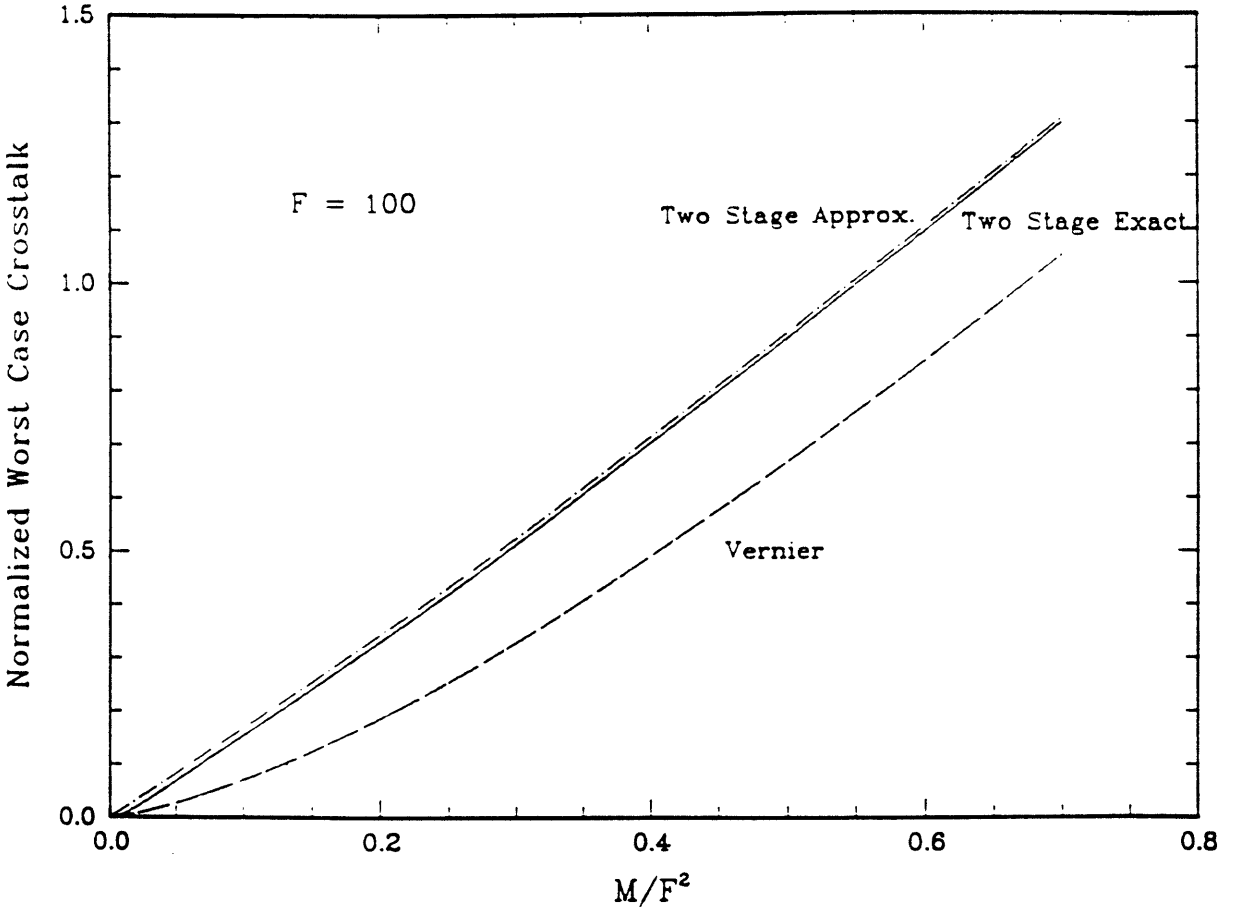
1.5
1.0
0.5
0.0
0.0
0.2
0.4
0.6
0.8
Normalized Worst Case Crosstalk
M/F²
F = 100
Two Stage Approx.
Two Stage Exact
Vernier

Fig. 14

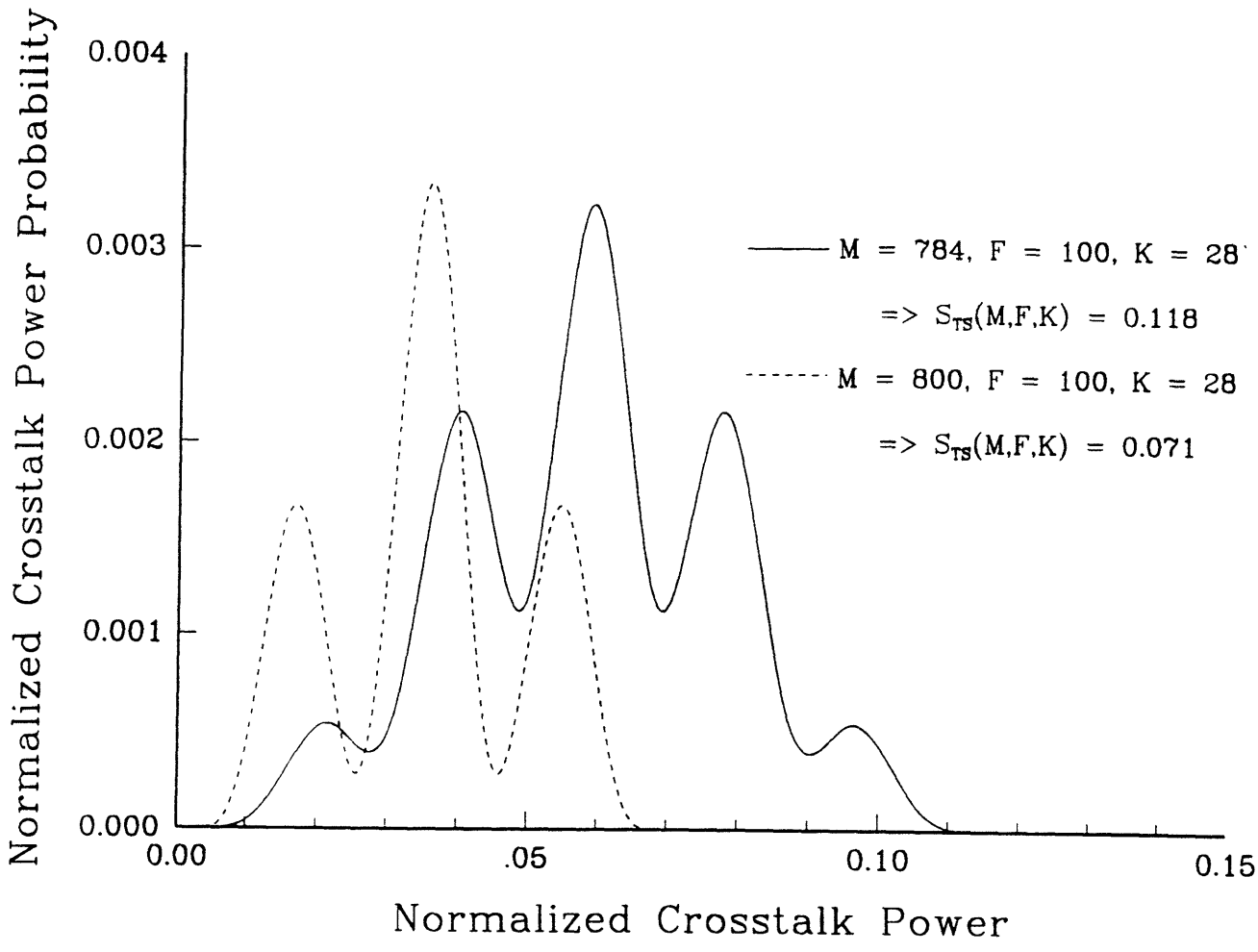
Normalized Crosstalk Power Probability
0.004
0.003
0.002
0.001
0.000
0.00
.05
0.10
0.15
Normalized Crosstalk Power
M = 784, F = 100, K = 28
=> $S_{TS}(M,F,K)$ = 0.118
M = 800, F = 100, K = 28
=> $S_{TS}(M,F,K)$ = 0.071

Fig. 15

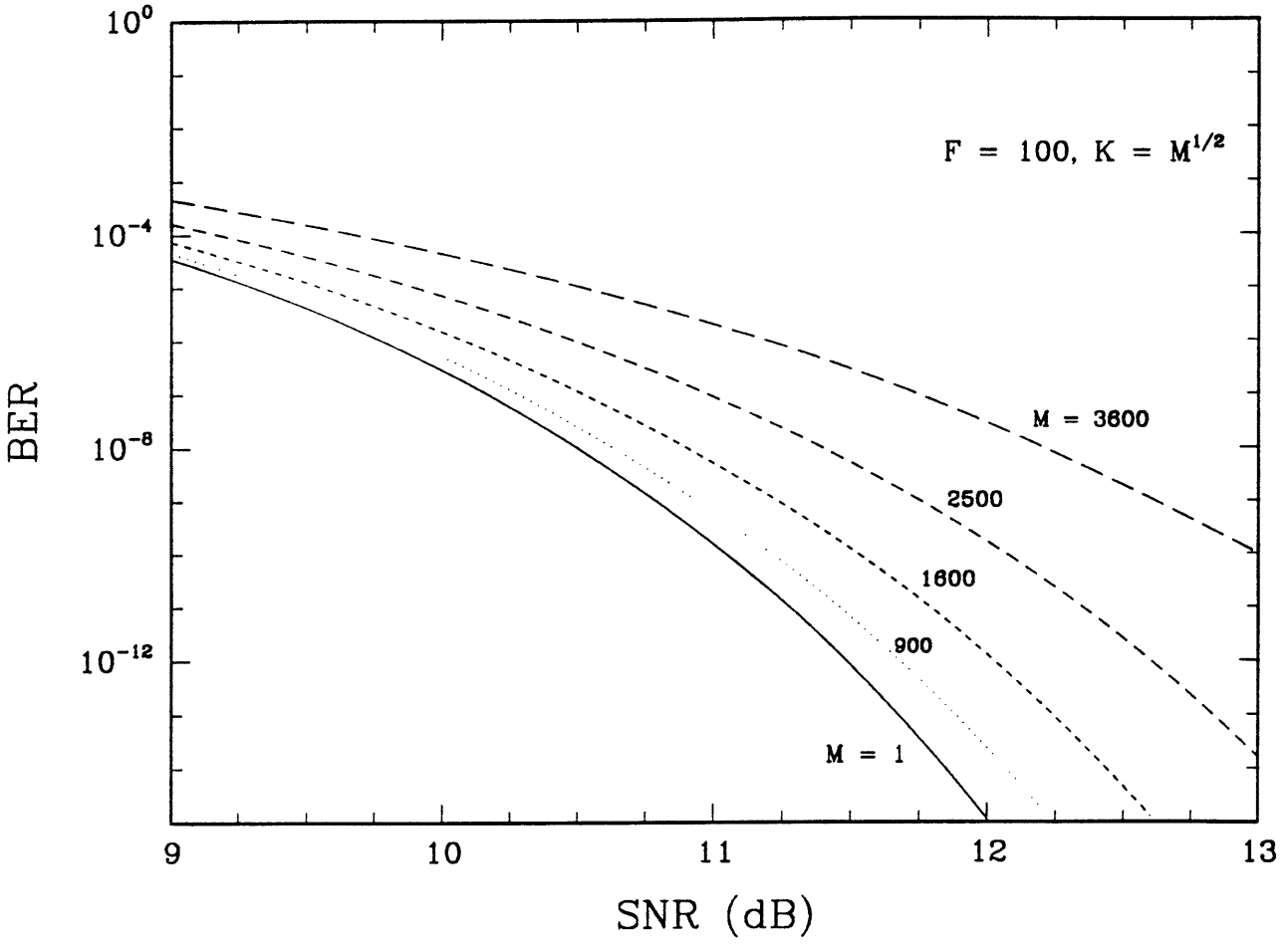
10^0
10^{-4}
10^{-8}
10^{-12}
BER
F = 100, K = $M^{1/2}$
M = 3600
2500
1600
900
M = 1
9
10
11
12
13
SNR (dB)

Fig. 16

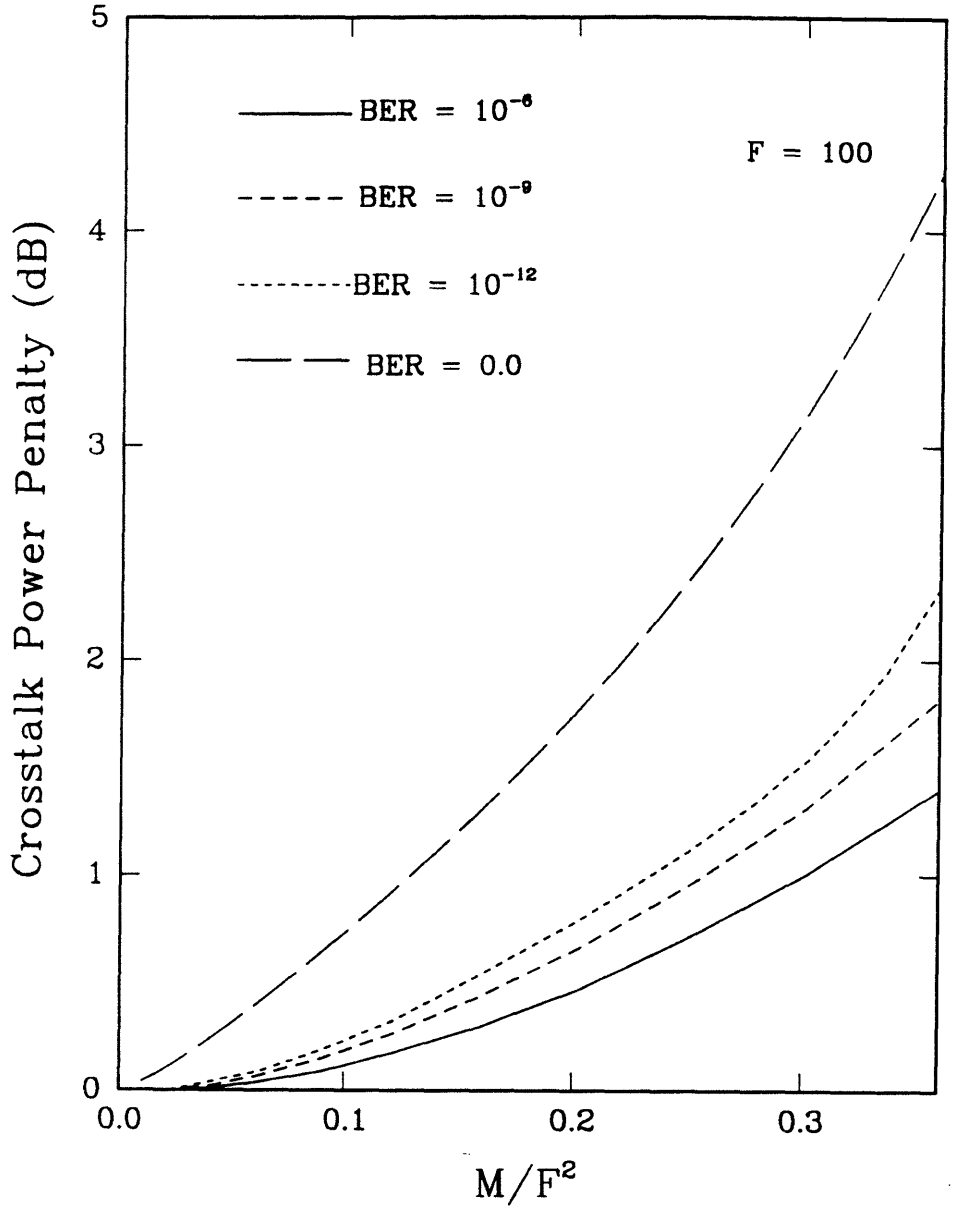
BER = 10^{-6}
BER = 10^{-9}
BER = 10^{-12}
BER = 0.0
F = 100
Crosstalk Power Penalty (dB)
0
1
2
3
4
5
0.0
0.1
0.2
0.3
M/F^2

Fig. 17

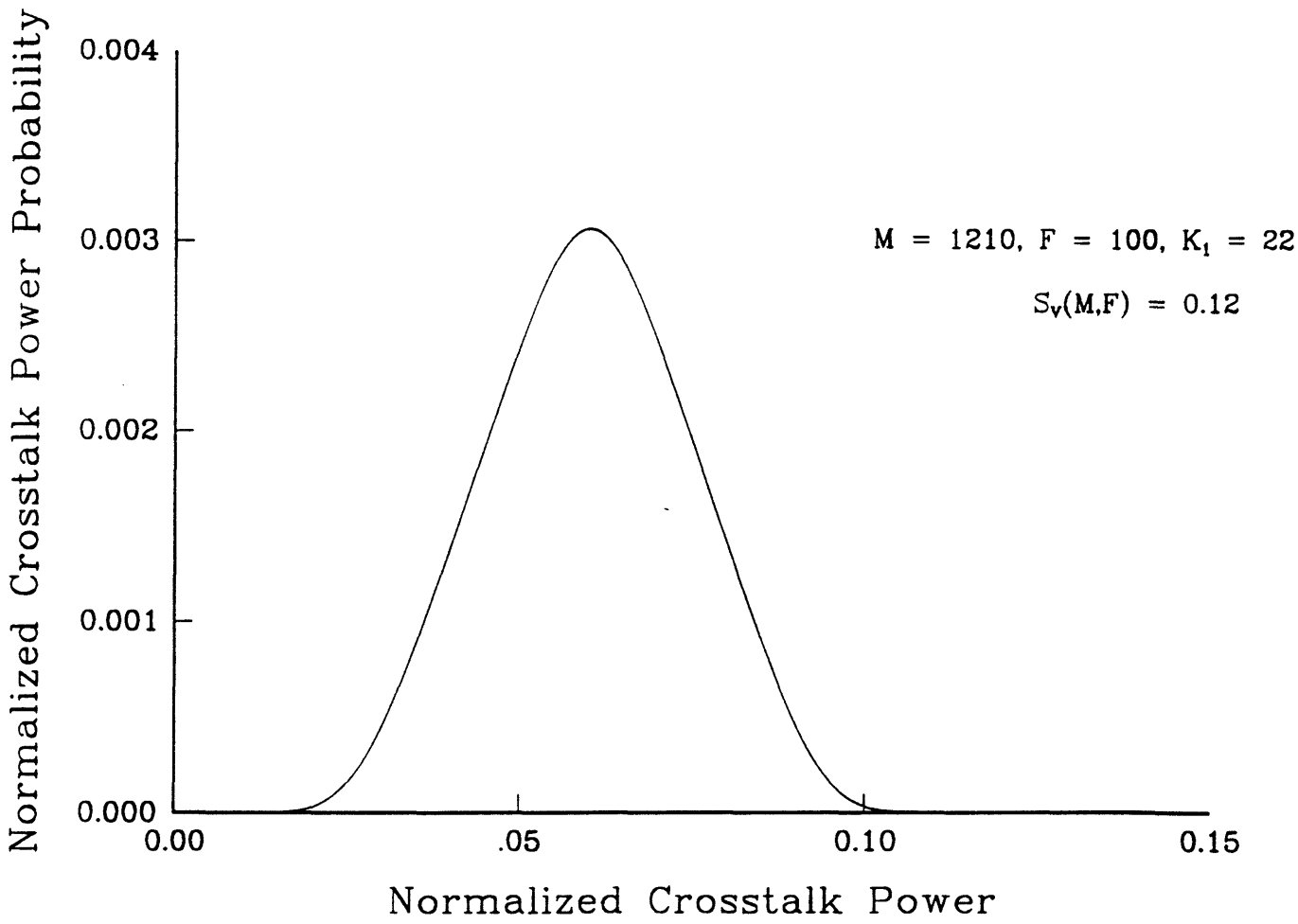
Normalized Crosstalk Power Probability
0.004
0.003
0.002
0.001
0.000
0.00
.05
0.10
0.15
Normalized Crosstalk Power
M = 1210, F = 100, K1 = 22
Sv(M,F) = 0.12

Fig. 18

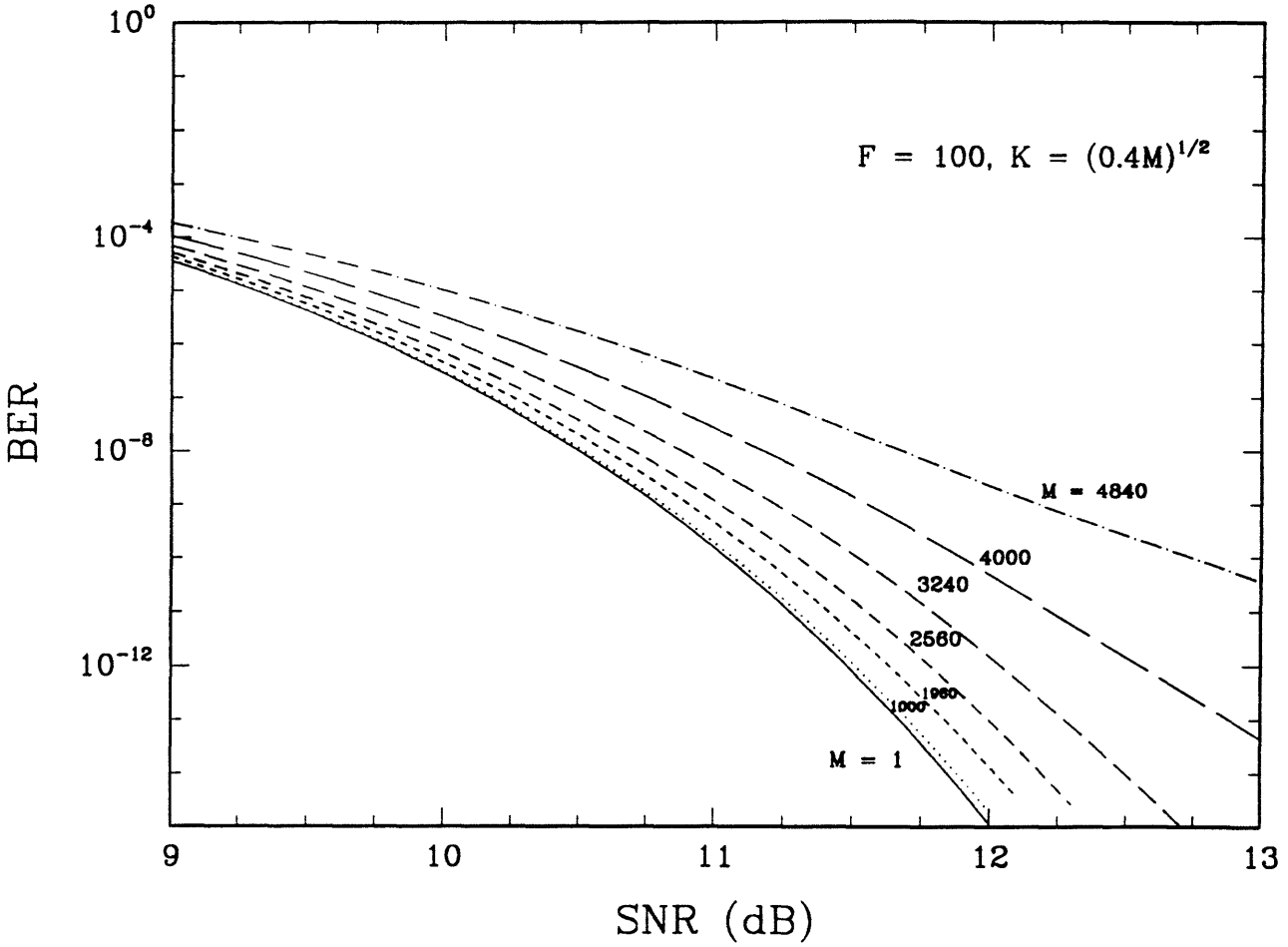
10^0
10^{-4}
10^{-8}
10^{-12}
BER
F = 100, K = $(0.4M)^{1/2}$
M = 4840
4000
3240
2560
1960
1000
M = 1
9
10
11
12
13
SNR (dB)

Fig. 19

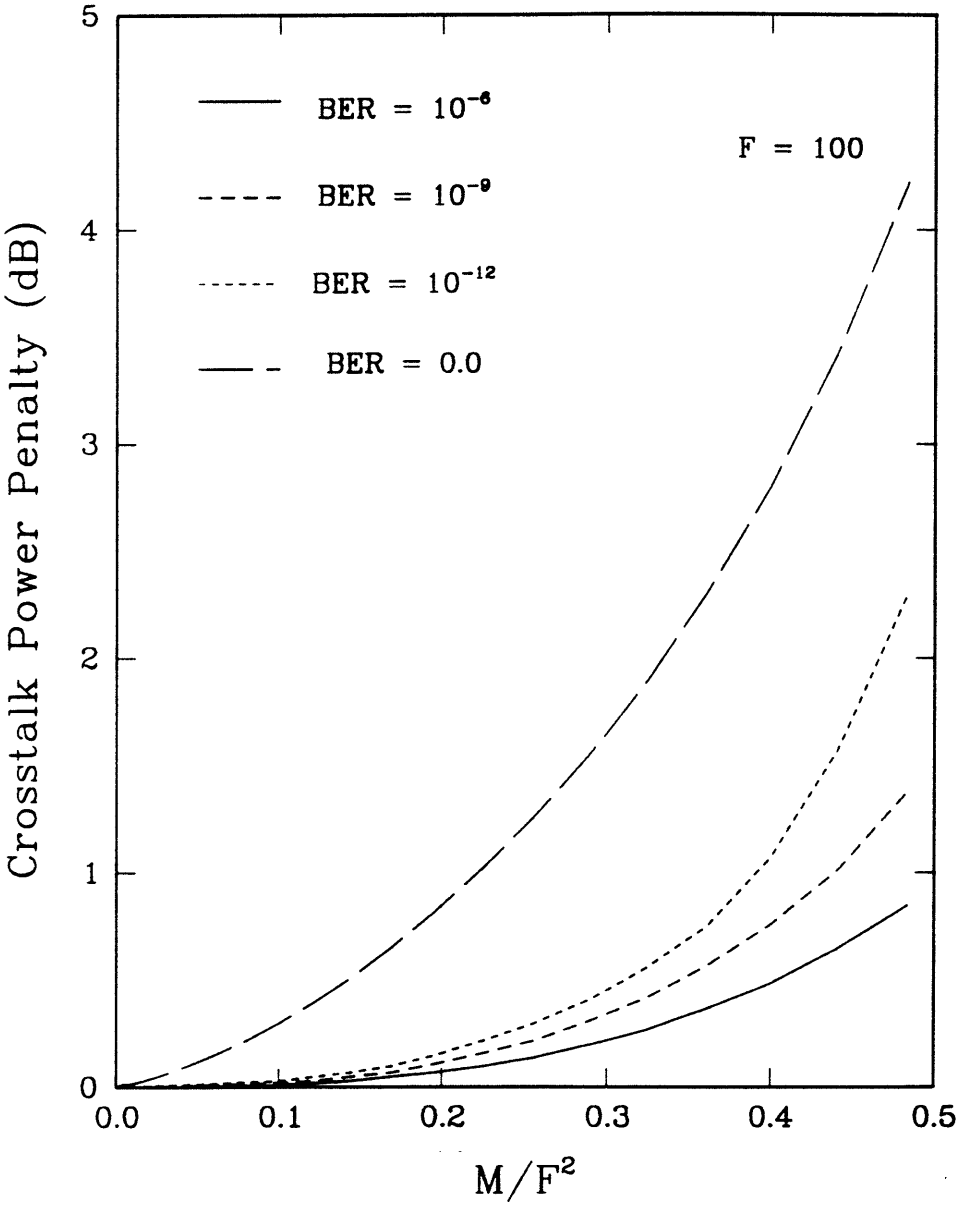
Crosstalk Power Penalty (dB)
5
4
3
2
1
0
0.0
0.1
0.2
0.3
0.4
0.5
M/F²
BER = 10⁻⁶
BER = 10⁻⁹
BER = 10⁻¹²
BER = 0.0
F = 100

Fig. 20

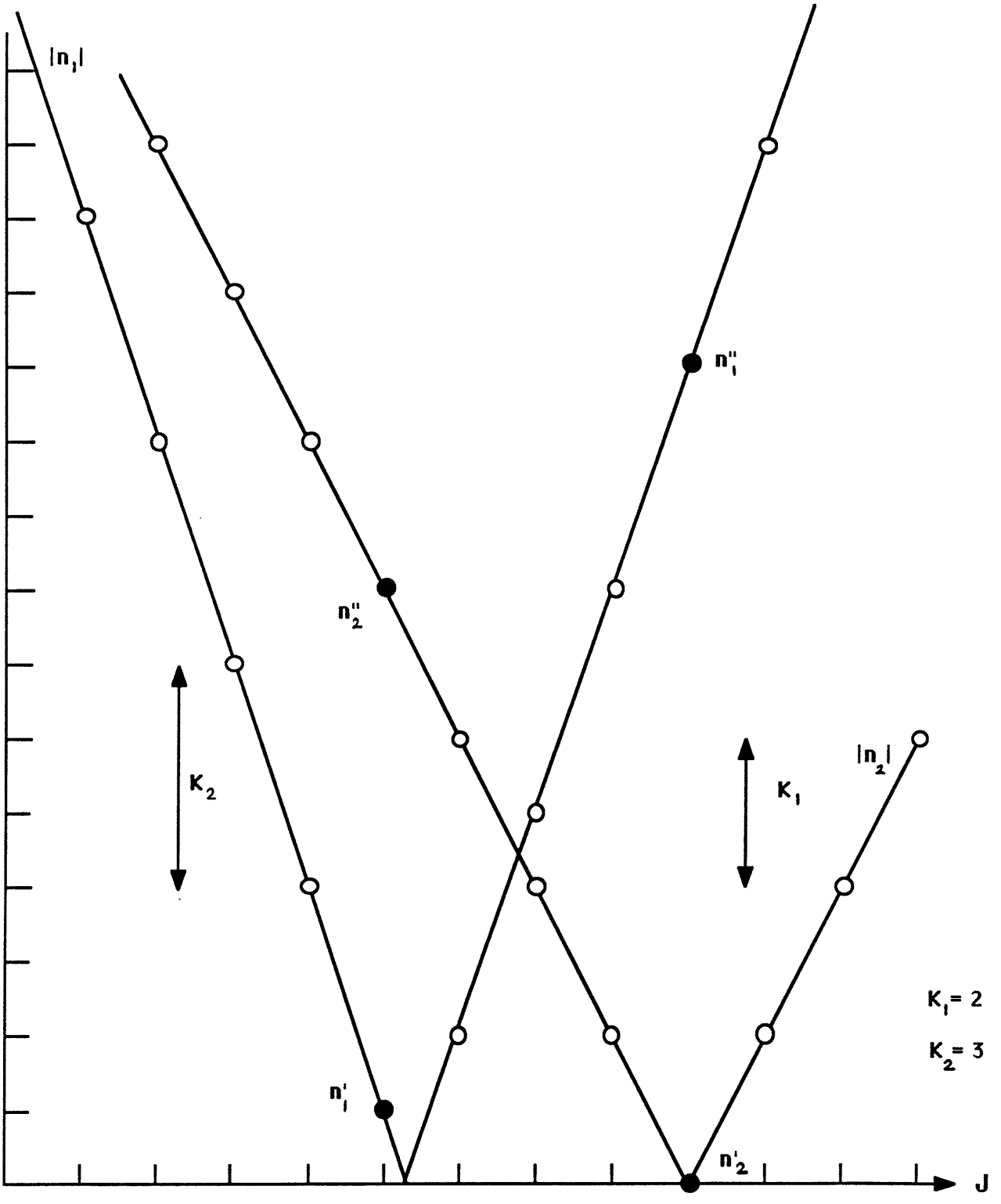

Fig. 21

Filter	Max. M	$F = 100$	$F = 300$
Single-Cavity	$M = 0.65F$	65	195
Double-Pass	$M = 1.4F$	140	420
Two-Stage	$M = 0.25F^2$	2500	22500
Vernier	$M = 0.44F^2$	4400	39600

Table I.